Global Biogeochemical Cycles

RESEARCH ARTICLE
10.1029/2018GB006009

Very Strong Atmospheric Methane Growth in the 4 Years 2014–2017: Implications for the Paris Agreement

E. G. Nisbet[1], M. R. Manning[2], E. J. Dlugokencky[3], R. E. Fisher[1], D. Lowry[1], S. E. Michel[4], C. Lund Myhre[5], S. M. Platt[5], G. Allen[6], P. Bousquet[7], R. Brownlow[8], M. Cain[9,10], J. L. France[1,11], O. Hermansen[5], R. Hossaini[12], A. E. Jones[11], I. Levin[13], A. C. Manning[14], G. Myhre[15], J. A. Pyle[16], B. H. Vaughn[4], N. J. Warwick[16], and J. W. C. White[4]

[1]Department of Earth Sciences, Royal Holloway, University of London, Egham, Surrey, UK, [2]Climate Change Research Institute, School of Geography Environment and Earth Sciences, Victoria University of Wellington, Wellington, New Zealand, [3]Earth System Research Laboratory, Global Monitoring Division, US National Oceanic and Atmospheric Administration, Boulder, CO, USA, [4]Institute of Arctic and Alpine Research, University of Colorado, Boulder, CO, USA, [5]NILU-Norwegian Institute for Air Research, Kjeller, Norway, [6]Centre for Atmospheric Science, University of Manchester, Manchester, UK, [7]Laboratoire des Sciences du Climat et de l'Environnement, Gif-sur-Yvette Cedex, France, [8]Energy and Sustainability Research Institute, University of Groningen, Groningen, Netherlands, [9]Environmental Change Institute, School of Geography and the Environment, University of Oxford, Oxford, UK, [10]Oxford Martin School, University of Oxford, Oxford, UK, [11]British Antarctic Survey, Cambridge, Cambs., UK, [12]Lancaster Environment Centre, Lancaster University, Lancaster, UK, [13]Institut für Umweltphysik, Heidelberg University, Heidelberg, Germany, [14]Centre for Ocean and Atmospheric Sciences, School of Environmental Sciences, University of East Anglia, Norwich, Norfolk, UK, [15]CICERO Centre for International Climate Research, Oslo, Norway, [16]National Centre for Atmospheric Science, and Department of Chemistry, University of Cambridge, Cambridge, UK

Key Points:
- Atmospheric methane is rising; its carbon isotopic ratio has become more depleted in C-13
- The possible causes of the change include an increase in emissions, with changing relative proportions of source inputs, or a decline in methane destruction, or both
- If this rise continues, there are significant consequences for the UN Paris Agreement

Supporting Information:
- Supporting Information S1

Correspondence to:
E. G. Nisbet, M. R. Manning, and E. J. Dlugokencky,
e.nisbet@rhul.ac.uk;
martin.manning@vuw.ac.nz;
ed.dlugokencky@noaa.gov

Citation:
Nisbet, E. G., Manning, M. R., Dlugokencky, E. J., Fisher, R. E., Lowry, D., Michel, S. E., et al. (2019). Very strong atmospheric methane growth in the 4 years 2014–2017: Implications for the Paris Agreement. *Global Biogeochemical Cycles*, *33*, 318–342. https://doi.org/10.1029/2018GB006009

Received 28 JUN 2018
Accepted 31 JAN 2019
Accepted article online 5 FEB 2019
Published online 18 MAR 2019

Abstract Atmospheric methane grew very rapidly in 2014 (12.7 ± 0.5 ppb/year), 2015 (10.1 ± 0.7 ppb/year), 2016 (7.0 ± 0.7 ppb/year), and 2017 (7.7 ± 0.7 ppb/year), at rates not observed since the 1980s. The increase in the methane burden began in 2007, with the mean global mole fraction in remote surface background air rising from about 1,775 ppb in 2006 to 1,850 ppb in 2017. Simultaneously the $^{13}C/^{12}C$ isotopic ratio (expressed as $\delta^{13}C_{CH4}$) has shifted, has shifted, now trending negative for more than a decade. The causes of methane's recent mole fraction increase are therefore either a change in the relative proportions (and totals) of emissions from biogenic and thermogenic and pyrogenic sources, especially in the tropics and subtropics, or a decline in the atmospheric sink of methane, or both. Unfortunately, with limited measurement data sets, it is not currently possible to be more definitive. The climate warming impact of the observed methane increase over the past decade, if continued at >5 ppb/year in the coming decades, is sufficient to challenge the Paris Agreement, which requires sharp cuts in the atmospheric methane burden. However, anthropogenic methane emissions are relatively very large and thus offer attractive targets for rapid reduction, which are essential if the Paris Agreement aims are to be attained.

Plain Language Summary The rise in atmospheric methane (CH_4), which began in 2007, accelerated in the past 4 years. The growth has been worldwide, especially in the tropics and northern midlatitudes. With the rise has come a shift in the carbon isotope ratio of the methane. The causes of the rise are not fully understood, and may include increased emissions and perhaps a decline in the destruction of methane in the air. Methane's increase since 2007 was not expected in future greenhouse gas scenarios compliant with the targets of the Paris Agreement, and if the increase continues at the same rates it may become very difficult to meet the Paris goals. There is now urgent need to reduce methane emissions, especially from the fossil fuel industry.

1. Introduction

Methane is the second most important anthropogenic greenhouse gas (M. R. Allen et al., 2018; Etminan et al., 2016; G. Myhre et al., 2013). In the 1990s, the atmospheric methane burden trended toward equilibrium, which it reached by the end of the twentieth century (Dlugokencky et al., 2011), with little or no growth in its atmospheric burden in the early years of this century. In 1984, the first year with detailed records, the global annual average atmospheric mole fraction of methane in the remote

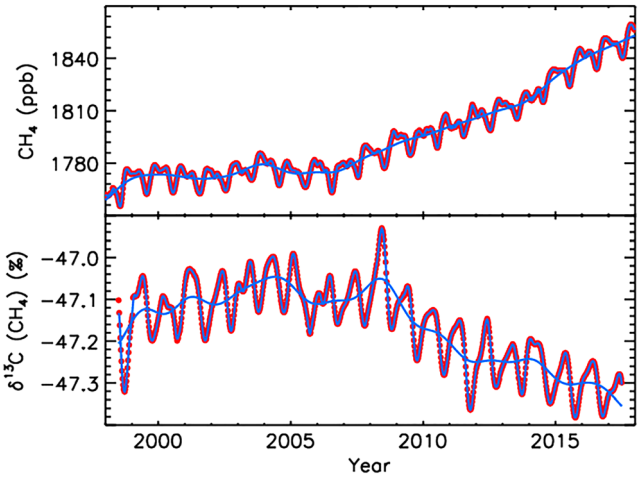

Figure 1. Atmospheric methane at Earth's surface in the remote marine troposphere (see Dlugokencky et al., 1994, for methods). Upper panel shows globally averaged surface atmospheric CH_4 at weekly resolution (red and blue) and deseasonalized trend (blue), 2000–2017. Lower panel as above, but for globally averaged surface atmospheric $\delta^{13}C_{CH4}$. Data from NOAA (see section 2). The *x* axis tick marks denote the 1st of January of the year indicated.

marine boundary layer was 1,645 ppb. In 2006, just before the recent growth phase began, it was about 1,775 ppb. This grew rapidly to an annual global mean of 1,850 ppb in 2017, a total rise of about 75 ppb in the 2007–2017 period (Figure 1). The increase is continuing. The growth in the mole fraction of methane in Arctic air was strong in late 2007, but since then in many years the strongest growth has been in the tropics and subtropics of the Northern and Southern Hemispheres (Figure 2). Overall, since 2007, methane growth has been sustained globally. Preindustrial methane was about 720 ppb around 1750 C.E. (Etheridge et al., 1998); thus, the decade of recent growth is equivalent to more than 6% of total growth to date since industrialization began.

Since 2007, atmospheric methane's changing carbon isotope ratio (expressed as $\delta^{13}C_{CH4}$) implies there has also been a significant change in the balance of sources and sinks. In contrast to the 1980s, and indeed the past two centuries, when $\delta^{13}C_{CH4}$ showed a sustained shift to more positive values indicative of gas leaks and coal emissions (Lowe et al., 1994; Rice et al., 2016), the present rise has been accompanied by a sustained shift in $\delta^{13}C_{CH4}$ to more negative values (Figure 2; Nisbet et al., 2016; Schaefer et al., 2016). Several hypotheses, not mutually exclusive, are possible to explain the changes. They are summarized here and then discussed in detail below (section 6):

1. An increase has occurred in isotopically very negative biogenic emissions, whether from wetlands or ruminants or waste, or all of these. If so, an increase in the proportion of global emissions from microbial sources may have driven both the increase in the methane burden and the shift in $\delta^{13}C_{CH4}$ (Nisbet et al., 2016; Schaefer et al., 2016).
2. Or, a strong rise in methane emissions from the use of natural gas and oil has taken place (Hausmann et al., 2016). Fossil fuel methane emissions are mostly somewhat more positive in $\delta^{13}C_{CH4}$ than −47‰ to −53‰. Thus, this hypothesis is only consistent with the observed isotopic shift if either (a) the new fossil fuel emissions have $\delta^{13}C_{CH4}$ markedly more negative than −47‰; or (b) if there has been a concurrent decline in a source of much more ^{13}C rich emissions, such as from biomass burning (Worden et al., 2017); or (c) both changes have occurred. Note that it is possible that both hypotheses (1) and (2) may be valid: that both microbial and fossil fuel emissions have increased. This would explain the observations, provided the increase in microbial emissions is sufficiently larger than that in fossil fuels, so that the bulk $\delta^{13}C_{CH4}$ value of the total source has become more negative.
3. Or the oxidative capacity—the cleansing power—of the atmosphere has declined, and hence the destruction of methane has slowed. A change in methane destruction has strong isotopic impact. If this hypothesis is correct, total emissions may have changed little or (less likely) even decreased, if the isotopic shift has been caused by a reduction in the OH sink (Rigby et al., 2017; Turner et al., 2017). However, Naus et al. (2019), using output from 3-D model simulations, pointed out the limitations of two-box modeling. They found only small differences in OH anomalies (up to 1.3%, averaged over 1994–2015) relative to the full uncertainty envelope (5–8%).

Although methane's apparent equilibration in the early years of this century was perhaps only a temporary pause in the human-induced secular increase in atmospheric methane (Bousquet et al., 2006), the renewed strong methane growth that began in 2007 (Nisbet et al., 2014, 2016) was so unexpected that it was not considered in pathway models preparatory to the Paris Agreement (M. Collins et al., 2013; Meinshausen et al., 2011; Moss et al., 2008; Rogelj et al., 2012). The current growth has now lasted over a decade. If growth continues at similar rates through subsequent decades, evidence presented here demonstrates that the extra climate warming impact of the methane can significantly negate or even reverse progress in climate mitigation from reducing CO_2 emissions. This will challenge efforts to meet the target of the 2015 UN Paris Agreement on Climate Change, to limit climate warming to 2 °C.

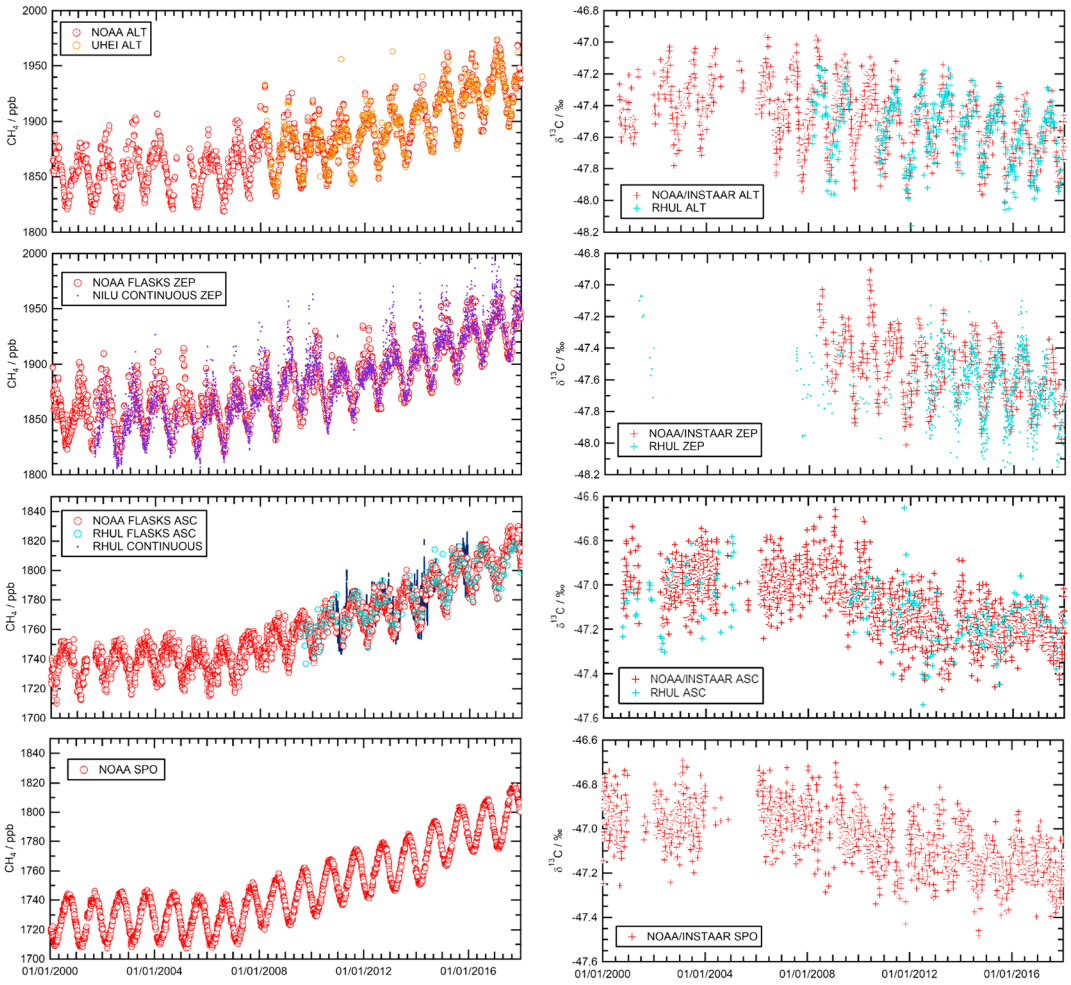

Figure 2. Methane from Arctic, equatorial, and Antarctic sites. Left: Mole fraction. Right: $\delta^{13}C_{CH4}$. Top: Methane at Alert, Canada (ALT; 82°N). Upper middle: Methane at Zeppelin, Svalbard. (ZEP; 79°N). Lower middle: Methane at Ascension (ASC; 8°S). Bottom: Methane at the South Pole (SPO). NOAA = National Oceanic and Atmospheric Administration; NILU = Norwegian Institute for Air Research; RHUL = Royal Holloway, University of London; INSTAAR = Institute of Arctic and Alpine Research; UHEI = University of Heidelberg and RHUL.

2. Methods

This paper focuses on direct in situ measurements of air. Air samples from remote sites reported here come from two groups of sources. Weekly air samples are collected in flask pairs at ~60 sampling sites in the Cooperative Global Air Sampling Network of the National Oceanic and Atmospheric Administration (NOAA), United States, a component of their Global Greenhouse Gas Reference Network. Air sampling, analysis, and data smoothing methods for methane are described in Dlugokencky et al. (1994). All methane measurements are reported on the WMO X2004A scale (Dlugokencky et al., 2005; www.esrl.noaa.gov/gmd/ccl/ch4_scale.html) in mole fraction units, nanomole per mole of dry air, or parts per billion, abbreviated as "ppb." Uncertainties range from approximately ±3 ppb in the early 1980s to approximately ±1 ppb in 2017 as measurement precisions have improved. A subset of NOAA samples is analyzed for $\delta^{13}C_{CH4}$; analysis methods are described in J. B. Miller et al. (2002); see also White et al. (2017).

The second data set is from the flask sampling program of the Greenhouse Gas Laboratory at Royal Holloway, University of London (RHUL) and the Norwegian Institute for Air Research (NILU) as well as from RHUL's cavity-ring-down absorption spectrometer operating on Ascension Island, United Kingdom, and NILU's measurement at Zeppelin, Svalbard (Spitsbergen). For methods, see Nisbet et al.

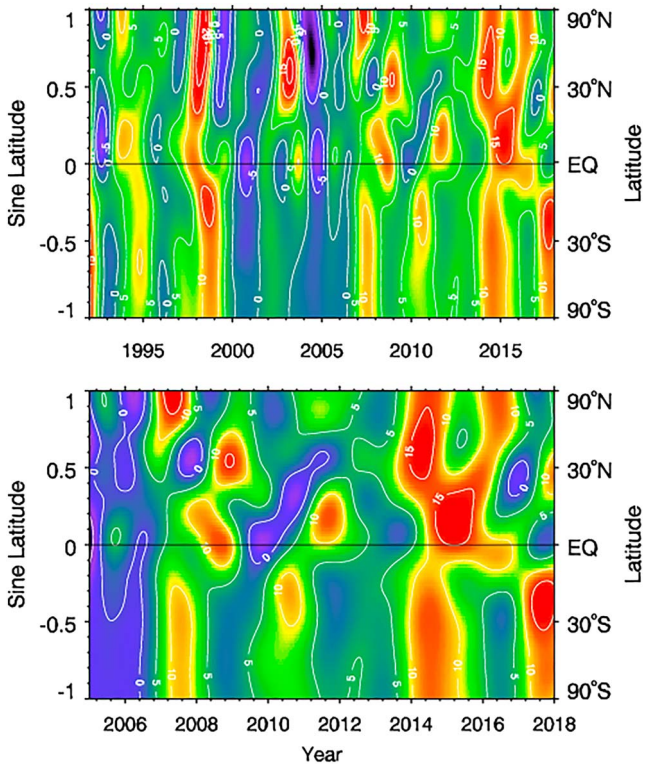

Figure 3. Zonally averaged CH_4 growth rate versus sine-of-latitude (equal area) and time: Figure 3 (upper) 1992–2018. Figure 3 (lower) Shows detail for 2005–2018.

(2016) and Fisher et al. (2006 and 2017). The RHUL time series were collected under a variety of projects supported by the European Union and the U.K. Natural Environment Research Council, and most recently the Natural Environment Research Council "MOYA" Global Methane Budget project, with help from Environment Canada and the University of Heidelberg (UHEI; samples from Alert), NILU (Zeppelin), the U.K. Met Office (Ascension), and the South African Weather Service (Cape Point).

All air samples from remote sites are analyzed in the laboratories in Boulder, Colorado (NOAA and the Institute of Arctic and Alpine Research [INSTAAR]) and London (RHUL). Mole fraction measurements are traceable to the WMO X2004A scale for both NOAA and RHUL (see Dlugokencky et al., 2005). Intercomparison of isotopic measurement ($\delta^{13}C_{CH4}$) between the INSTAAR and RHUL laboratories is by exchange of high pressure cylinders of air as detailed in Umezawa et al. (2018) and in Nisbet et al. (2016). $\delta^{13}C_{CH4}$ repeatability is approximately ±0.06‰ (INSTAAR) and ±0.05‰ (RHUL).

3. Results

Atmospheric methane grew very strongly in 2014–2017 (Figure 1 upper panel). Methane's growth in 2014 was a remarkable 12.7 ± 0.5 ppb, and, unusual for the record, the distribution of annual growth was global (Figures 2 and 3). Further very strong increases in 2015 (10.1 ± 0.7 ppb), 2016 (7.0 ± 0.7 ppb), and 2017 (7.7 ± 0.7 ppb) added to the methane burden already measured in 2014 (values based on NOAA CH_4 Trends: www.esrl.noaa.gov/gmd/ccgg/trends_ch4/, accessed October 2018). Sustained annual growth of about 10 ppb over the 4-year period was last observed in the 1980s, when the Soviet Union's gas industry was developing very rapidly. The ~13 ppb increase in 2014 ranks among the very highest annual increments in the measured record.

Concurrently with the renewed growth since 2007, $\delta^{13}C_{CH4}$ has become significantly more negative by about 0.3‰ (Figure 1, lower panel). Overall globally, the bulk $\delta^{13}C_{CH4}$ ratio has shifted more negative by about −0.03‰/year (see also Nisbet et al., 2016). This isotopic trend to more negative values, which has now been observed globally for more than a decade (Figure 1), reverses the sustained positive trend over the nineteenth and twentieth centuries (Francey et al., 1999).

The global nature of the changes is shown in Figure 2, from Alert (82°N) in the Canadian Arctic and Zeppelin (79°N), in Svalbard (Spitsbergen), both in the high Arctic; Ascension Island (8°S), just south of the equator in the remote central mid-Atlantic; and from the South Pole. Measurement data are shown without fitted curves to guide (and train) the eye, so that the reader can make an uninfluenced judgment on trends. Our measurements from all four stations are in agreement that the mole fraction of methane has risen, and that the $\delta^{13}C_{CH4}$ ratio has fallen significantly since 2007. However, since 2014, there is significant latitudinal variation in mole fraction and $\delta^{13}C_{CH4}$ trends (Figures 2 and 3), indicating a more complex regional picture. Most recently, over 2014–2017, in parallel with growth in the mole fraction of methane, the isotopic shift has continued in high northern latitudes, and also in Antarctica (see Figure 2, right panels). At Ascension Island, however, $\delta^{13}C_{CH4}$ fell in 2012 and in 2014, whereas in 2015 and 2016 the values stabilized (Figure 2c), with possible signs of resumed decline in 2017.

The *x* axis tick marks denote the 1st of January of the year indicated. Note that both NOAA and RHUL results are similar, so trends are not single-lab artifacts. Measurements from NOAA/INSTAAR and RHUL, with additional flask samples from NILU (Zeppelin), and UHEI Institut für Umweltphysik (Alert), and RHUL/U.K. Met Office (Ascension). Note that *y* axis ranges differ in different panels. Data are shown without guiding fits, so the reader can judge trends unguided.

4. Extreme Growth in 2014, 2015, 2016, and 2017: Latitudinal Analysis by Zones

During the 4-year period 2014–2017, methane growth was sustained, each year bringing a major increment upon the remarkable growth of the previous year. Figure 3 shows contours of zonally averaged CH_4 growth rate (ppb/year) in the surface troposphere versus sine of latitude and time. The sine-latitude plot is proportional to surface area and thus represents the global significance of each latitude zone. Methane mixes across the planetary troposphere in about a year and its lifetime is less than a decade (Dalsøren et al., 2016; Dlugokencky et al., 2011; Lelieveld et al., 1998). In the late 20th and early 21st century pattern (Dlugokencky et al., 2011, 1994; Nisbet et al., 2016), single years of strong regional methane growth were typically followed by declines to the global background, as methane mixed from the surface, where it is measured, throughout the troposphere. In marked contrast, recent year-to-year growth has been so strong that growth has been recorded everywhere. Thus, in the post-2000 context, 2014–2017 is very unusual, with few pronounced short-lived zonally averaged declines (Figure 3: for methodology see the supporting information).

One hypothesis is that this growth has been driven by increased emissions. Regional pulses of strong seasonal emissions, whether from seasonal wetlands or during periods of high winter production from gas extraction, will disperse meteorologically in succeeding periods. As transport distributes emission pulses across the globe, strong growth years observed in specific latitude zones will likely be followed by short episodes of decline as regional emissions wax and wane, with atmospheric transport mixing the methane globally, including vertically, away from the surface where most observations are made.

Alternatively, if the growth in the mole fraction of methane has been driven by a decline in sinks, then the impact would be expected to be most marked in the tropical midtroposphere, where methane destruction is most intense (e.g., see Table 1 below). The effects of reduced destruction would thus be likely to be most immediately observable in the tropics, but note that mid-troposphere air can travel far before interacting with the remote sites of the observation network, which mostly sample the marine boundary layer.

Figure 3 (upper part) shows the methane growth rate from 1992 to 2018, from NOAA data. The figure includes, from 1992 to 2000, the later years of the long period of sustained growth that was observed from the early 1980s (when the global measurement network began) through to the end of the century. Then came the period of stability, growth in some years, decline in others, from the millennium until 2007. Strong growth resumed in 2007, becoming stronger from 2014. Figure 3 (lower part) is the same as Figure 3 upper, but in detail showing the shorter time period 2005–2018. During the later years of the period of stability that lasted from the millennium, growth occurred in some years, decline in others. Strong growth resumed in 2007. Then, in the years from 2014, the focus of this report, the figure clearly shows the sharp increase in the growth rate.

Contours of growth rate (white lines) are shown every 5 ppb/year. Warm colors show growth; cool colors decline. In this equal area plot note the importance of the zonal band under the sweep of the Intertropical Convergence Zone (very roughly sin lat. 0.45 to −0.4). The Arctic and Boreal zones are above 0.8 sin lat. Note also that the contouring, which is based on deseasonalized trends, does not faithfully reproduce the timing of changes, and there are important end-effects. Thus, the figure should be seen as illustrative, not definitive, especially in the past year. Data from NOAA.

4.1. Methane in the Arctic and Boreal Zone (North of ~50°N)

The mole fraction of methane grew strongly in the zone north of 50°N in the 4-year period between 2014 and 2017. In 2014, zonal growth as measured at NOAA's network of sampling sites (Dlugokencky et al., 2017; White et al., 2017) was high (>13 ppb) but the focus of higher growth was further south, around 40°N. Growth in 2015 was led by the northern tropics and the Arctic/Boreal zone lagged the rest of the world, but in 2016 the zone north of 50°N had the highest growth rate (>12 ppb) globally (Figure 3). Then in 2017, growth was focused in the Southern Hemisphere and the Arctic/Boreal zone again lagged. The Alert and Zeppelin $\delta^{13}C_{CH4}$ records in 2014–2016 (Figure 2) show a continuation of the post-2007 shift to more negative $\delta^{13}C_{CH4}$ values (reported by Nisbet et al., 2016). In the entire post 2007 period, overall methane growth, measured at Environment Canada's Alert station and at NILU's Zeppelin station, was strong in the Arctic zone in mid-to-late 2007, but then growth in the latitudinal zone north of 50°N, though steady, tended to lag the rest of the world from 2008 until 2014, when growth was strong throughout the

extratropical Northern Hemisphere, and again in 2016, but not in 2017 (Figure 3). Unfortunately, $^{14}CH_4$ and CH_3D monitoring are too limited to build a global picture.

Regional high-latitude emissions are primarily from wetlands in summer and gasfields in winter (Berchet et al., 2016; Fisher et al., 2011, 2017; France et al., 2016), though cold season wetland emissions may be more important than previously thought (Zona et al., 2016). There is no strong evidence for very large emissions from hydrates (Berchet et al., 2016; C. L. Myhre et al., 2016). It should be noted also that at high latitudes the OH methane sink is relatively weak (see Table 1 below) and atmospheric transport is rapid and largely horizontal (Bousquet et al., 2011), thus changes in emissions have a more pronounced short-term impact on the zonal burden than at lower latitudes. As much of this region is warming disproportionately in global climate warming (Pitham & Mauritsen, 2014), Arctic and Boreal zone emissions would be expected to be responding sharply to increased warmth, but in the dryness and warmth, microbial soil methanotrophy would also be favored. Nearly three decades of measurement at Barrow, Alaska, have shown little change in seasonal methane enhancements from the land sector, despite a significant increase in annual mean temperatures (Sweeney et al., 2016).

4.2. Methane in the Populated North (30 to ~50°N)

Mid-northern latitudes led the strong global rise in 2014, when zonal methane growth was above 14 ppb. Methane growth was again 10 ppb in 2016. More recently, growth in this zone has been subdued. The isotopic trend to more negative $\delta^{13}C_{CH4}$ began around 2005 and continued through the study period (see, e.g., records from Mace Head, Ireland (53°N), and Terceira, Azores (39°N), in the NOAA data set https://www.esrl.noaa.gov/gmd/dv/iadv/), suggesting that growth was not led by fossil fuel emissions (which have relatively enriched $\delta^{13}C_{CH4}$) even though gas and coal extraction is very significant in this latitudinal zone (Schwietzke et al., 2016; Sherwood et al., 2016, 2017).

Overall this century, despite the increase in fossil fuel extraction and use, methane growth in this latitudinal zone has varied, with episodes of decline in 2004, 2006, and 2008. Apart from the notable growth in 2014 and 2016, the other episode of growth was in 2003, during a summer of extreme heat in Europe and major fires in Siberia (Trigo et al., 2005).

4.3. Methane in the Tropics and Subtropics (30°N to 30°S)

Very strong methane growth (>10 ppb) took place in the tropics in 2014 and 2015; since then the tropical zonal annual growth rates remain high (around 8 ppb/year). In 2014, growth in the southern tropics was nearly 13 ppb, and in 2017 the growth in the southern tropics was extreme (>15 ppb). These changes to the zonal methane burden took place during the remarkable episode of year-on-year temperature warming increments that were sustained through 2014, 2015, and 2016 (Jiménez-Muñoz et al., 2016; UK Met Office, 2018; WMO, 2016). Overall, growth since 2007 has been sustained in both northern and southern tropics, with prior episodes of strong increase in 2007–2008 (nearly 10 ppb), and 2010 (9 ppb), before the 2014–2017 period. Thus, the tropics have played a major role in leading methane growth since 2007 (Figure 3), including during the 2015 El Niño.

As in the high north, the tropical $\delta^{13}C_{CH4}$ record at Ascension Island in the equatorial remote central Atlantic shows a significant shift to more negative values (Figure 2). Here the $\delta^{13}C_{CH4}$ shift, which began at the end of 2007, may have temporarily halted around 2013 to the end of 2016. Since the start of 2017, the trend appears to be shifting again to more negative values, but future years of data will be needed to confirm this resumption of the trend to more depleted values. It should be noted that there is a significant worldwide tropical sampling deficiency for XCH_4 and $\delta^{13}C_{CH4}$ measurement: for isotopes there is a critical lack of sustained multiyear tropical observational time series, which is arguably the weakest link in our understanding of global atmospheric methane. The only remote equatorial time series is from Ascension Island, which has almost invariant SE Trade winds from the deep South Atlantic, that later become the background input to Amazonian air masses.

4.4. Methane in the South (30 to 90°S)

In parallel with global trends, growth in this zone was >12 ppb in 2014, and 9 ppb in 2015. In 2016, growth dropped below 4 ppb, rising again in 2017 (>12 ppb). This zone has proportionately much less methane-producing land mass than other zones, but is significant for the impact of the Cl sink on the isotopic

budget. As in the rest of the world, a sustained negative $\delta^{13}C_{CH4}$ shift is also observed at the South Pole (Figure 2). Unlike the Arctic stations, South Pole is far from major sources (see Table 1 below). Thus, the South Pole time series portrays broad global trends: in contrast to the more variable Arctic record, the South Pole displays a smooth sustained trend to more negative $\delta^{13}C_{CH4}$ values throughout the period from 2007 to 2017, with the trend to more negative $\delta^{13}C_{CH4}$ becoming less pronounced since 2014.

5. Methane Sources and Sinks: The Insight From Carbon Isotopes

The various hypotheses to explain the current rise in methane are outlined in section 1: the causes driving the current strong rise in methane are not fully understood, and may include changes in both sources and sinks (Bousquet et al., 2011; Dalsøren et al., 2016; Nisbet et al., 2016; Rigby et al., 2017; Saunois et al., 2017; Schaefer et al., 2016; Schwietzke et al., 2016; Turner et al., 2017; Worden et al., 2017). Although at present insufficient, the information required to constrain the relative causes of methane's observed rise lies in the geographic and seasonal spreads in both mole fraction data for methane and in corresponding isotopic measurements (Figures 2 and 3).

The continuing negative trend in $\delta^{13}C_{CH4}$ that began in 2007 is particularly elucidating as it implies a profound change in the evolving global budget, contrasting sharply with the two centuries of sustained positive trend in $\delta^{13}C_{CH4}$. This earlier isotopic trend was sustained during methane's rapid nineteenth and twentieth century growth, contemporary with complex anthropogenic changes, that included fossil fuel emissions from natural gas, oil, and coal extraction, perhaps increased biomass burning with increasing tropical agricultural populations (Crutzen & Andreae, 1990), and wetland drainage, in parallel with increasing ruminant populations.

Background atmospheric $\delta^{13}C_{CH4}$ is currently around −47‰. Methane removal by atmospheric hydroxyl, OH imposes a kinetic isotope effect of around 3.9‰ (Saueressig et al., 2001) or 5.4‰ (Cantrell et al., 1990), which implies a bulk global emission $\delta^{13}C_{CH4}$ value from all sources contributing to the current burden of between −54‰ and −52‰ (Nisbet et al., 2016). However, interpretation of isotopic observations is complex, because of the multidecadal time scale of isotopic equilibration (Tans, 1997). In the short term, emissions with $\delta^{13}C_{CH4}$ between −47‰ and −53‰ initially help move the total atmospheric burden negative, but as the emissions are destroyed by OH, on a decadal time scale, the long-term effect is to move the bulk global burden positive. Thus, the sustained post-2007 negative isotopic shift, if driven primarily by an emission increase and over a long period, a decade or more, implies increasing emissions from sources more negative than about −53‰.

Methane sources vary with latitudinal zone. Isotopic signatures of sources are summarized by Dlugokencky et al. (2011) and in more detail by Sherwood et al. (2017), Zazzeri et al. (2016), and Brownlow et al. (2016). Much depends on vegetation type: temperate vegetation is mainly of C3 plants, which are very selective for ^{12}C. Tropical biomes, especially the savannas and wetlands, typically include abundant C4 grasses (e.g., papyrus). These evolved during low CO_2 periods and their carbon capture from the air is less selective against ^{13}C: thus, their biomass has higher ^{13}C contents. Globally, our knowledge of $\delta^{13}C_{CH4}$ signatures of methane released into open air is very inadequate (Feinberg et al., 2018).

Emissions from the Arctic and boreal zone north of 50°N come dominantly from widespread summer C3 wetlands ($\delta^{13}C_{CH4}$ about −70 ± 5‰) and also from releases, especially in winter, from the very large Arctic gas fields ($\delta^{13}C_{CH4}$ about −50 ± 5‰; Fisher et al., 2011, 2017; France et al., 2016). This region also hosts permafrost and gas hydrates, though emissions from gas hydrates and seeps currently seem to be lower than previously estimated (C. L. Myhre et al., 2016; Berchet et al., 2016; Thornton, Geibel, et al., 2016). Double-counting in emissions inventories may mean that Arctic high-latitude emissions have been overstated, and may currently be as low as roughly 4% of the global total (Thornton, Wik, et al., 2016), although regional inverse modeling suggests up to 15% of global methane emissions, both natural and anthropogenic (including the giant Siberian Arctic gas fields) come from the region north of 50°N (Thompson et al., 2017). The question of the region's significance on a global scale thus remains open.

Methane emissions in the zone from 50°N to the Tropic of Cancer include both strong biogenic and anthropogenic emissions. These come from extensive Russian and Canadian C3 wetlands ($\delta^{13}C_{CH4}$ approximately −65 ± 5‰); from the natural gas industry ($\delta^{13}C_{CH4}$ approximately −50‰ to −30‰), with much of the

world's production in the United States, Russia, and the Middle East; and from coal production ($\delta^{13}C_{CH4}$ approximately $-40 \pm 15‰$), especially in China. The $\delta^{13}C_{CH4}$ values given here are rough overall estimates based on Schwietzke et al. (2017), Brownlow et al. (2017), Zazzeri et al. (2016), and Ganesan et al. (2018).

China may have been responsible for up to 40% of global methane growth between 2003–2005 and 2007–2010 (Thompson et al., 2015) and was likely an important contributor to growth in the post-2014 years. In particular, using an atmospheric Bayesian inversion, Thompson et al. (2015) inferred that total emissions from all sources in East Asia grew from 43 ± 4 Tg in the year 2000 to 59 ± 4 Tg in 2011 much of which was because China's annual emissions grew from 39 ± 4 to 54 ± 4 Tg in the period. However, Feinberg et al. (2018) show that it is hard to reconcile inventory estimates of growth in Chinese coal production (e.g., EDGAR, 2017) with the observed isotopic trends, unless China is switching to lower quality coals with more negative $\delta^{13}C_{CH4}$.

In the South American and African tropics, globally significant wetland emissions occur (Melton et al., 2013). These are primarily from the Amazon and Pantanal wetlands, and in Africa from the Congo, Nile, Zambesian, and other C4 papyrus wetlands: their $\delta^{13}C_{CH4}$ signatures are poorly studied but likely approximately $-55 \pm 10‰$ (e.g., Brownlow et al., 2017). Emissions from tropical wetlands vary as wetland area responds to changes in precipitation and increase exponentially with temperature, provided water and nutrients are available (e.g., Gedney et al., 2004; McNorton, Gloor, et al., 2016; Westerman & Ahring, 1987). The $\delta^{13}C_{CH4}$ values of cattle breath also contribute to tropical methane emissions. These values are poorly studied and will depend on proportions of C4 fodder such as maize and sugar cane tops, but are likely similarly to be approximately $-55 \pm 10‰$ (e.g., Brownlow et al., 2017). Tropical cattle prosper in wet seasons.

Similarly, tropical Asia has abundant cattle (especially in India) and wetlands (Ganges Delta and S.E. Asia including Borneo), as well as extensive gas industries, and large-scale coal mining in India and Indonesia. It is possible that, as pointed out by Worden et al. (2017), a reduction of biomass burning emissions of a few Teragrams per year (Tg/yr) may have occurred and masked increasing fossil fuel-related emissions in the global emissions budget. This is discussed further below (section 8.2).

In the extratropical Southern Hemisphere, natural emissions are from cattle, biomass burning, and some wetlands, with significant industrial emissions from Australia (gas, coal; Zazzeri et al., 2016) and South Africa (coal).

Geological emissions also occur worldwide, but may be much smaller than hitherto estimated (Petrenko et al., 2017).

The main sink of atmospheric methane, destruction by atmospheric hydroxyl (OH), occurs especially in the bright moist tropical midtroposphere, where OH, which has a very short lifetime (~1 s), is most active. OH is thought to be well buffered, not sensitive to perturbations by natural or anthropogenic emission changes. OH interannual variability can have important impact on methane growth rates (e.g., see McNorton, Chipperfield, et al., 2016). As OH destruction is likely modulated by strong changes in meteorology (C. D. Holmes et al., 2013), such as may have taken place in the past decade in tropical midtropospheric moisture and cloud structure, it is possible that significant interannual variability in OH destruction may indeed occur, though detailed mechanisms capable of driving such large changes in the oxidative capacity of the atmosphere have not been proposed. However, in this context, Nicely et al. (2018) and Lelieveld et al. (2016) agreed with Montzka et al. (2011) in finding that interannual variability of OH has probably been fairly small.

The uncertainty in our understanding of OH is illustrated by the findings of Naus et al. (2019), who note a number of biases caused by using a box model, resulting from a combination of variations in transport and variations in source/sink distributions; when those biases are corrected using a 3-D model, they find an opposite trend in OH. In their work, the sensitivity of interannual OH anomalies to the biases is modest (1–2%), relative to the significant uncertainties on derived OH (5–8%). In an inversion implementing all bias corrections simultaneously, they did find a shift to a positive OH trend over the 1994–2015 period.

Reduced destruction by lesser sinks may also have contributed to the rise in the global methane burden (Nisbet et al., 2016). These smaller sinks include soil methanotrophy (A. J. Holmes et al., 1999; Serrano-Silva et al., 2014), caves in karst limestone topography (Mattey et al., 2013), and Cl from marine aerosols, especially in the Southern Hemisphere with its large oceans (Hossaini et al., 2016). Soil moisture and

hence methanotrophy vary with rainfall, temperature, and the height of a water table, so that drought can increase rates of consumption of atmospheric methane by a factor of >4 (Davidson et al., 2004). The Cl sink (Allan et al., 2007; Hossaini et al., 2016) is likely affected by varying wind conditions in the marine boundary layer.

6. Testing the Hypotheses That May Explain the Recent Rise in Methane

6.1. The Hypothesis That Biogenic Methane Emissions (Mainly From Wetlands and Cattle) Have Increased, While Destruction by OH Has Been Relatively Constant

The first hypothesis to explain the methane growth and negative $\delta^{13}C_{CH4}$ trend is that much of the 2014–2016 growth could have come from increased biogenic emissions, while destruction rates remained steady. Recent years have been very warm and increased emissions would be expected from widespread tropical wetlands, supplemented by expanding populations of tropical ruminants, well fed on good vegetation growth (Nisbet et al., 2016; Schaefer et al., 2016), and perhaps the rapid expansion of landfills, many unregulated, in the tropics. For example, Thompson et al. (2018) inferred that between 2006 and 2014 microbial sources increased by 35 ± 12 Tg/year, and fossil fuel sources by 13 ± 8 Tg/year, while biomass burning decreased by 3 ± 2 Tg/year and soil oxidation increased by 4 ± 6 Tg/year. If the hypothesis that growth is primarily driven by increasing emissions from biogenic sources is correct, then the continuing negative shift in 2014–2016 suggests further enhancement of the biogenic inputs.

The hypothesis that wetlands have led the recent growth is consistent with evidence for a post-2006 increase in wetland emissions (+3%), mainly from the Tropics (McNorton, Gloor, et al., 2016; Parker et al., 2018; Zimmermann et al., 2018). Moreover, there is substantial evidence for the expansion of the meteorological tropics, especially in summer (e.g., R. J. Allen et al., 2014; Davis & Birner, 2017). Ganesan et al. (2018) showed the need for better isotopic knowledge of tropical wetland emissions before the large uncertainties in fluxes derived from inversion models can be reduced. Using a spatially resolved source signature map, they found mean $\delta^{13}C_{CH4}$ of northern wetland methane emissions to be −67.8‰, and mean tropical wetland emissions to have $\delta^{13}C_{CH4}$−56.7‰.

The years 2014, 2015, and 2016 were of exceptional warmth, each year surpassing the previous as the warmest on record (Rahmstorf et al., 2017; WMO, 2016). The extreme 2014 methane growth event took place in a year that was 0.99 °C warmer compared to 1880–1909 conditions (NCDC, 2017). In 2015 (1.13 °C warmer than 1880–1909 conditions) the extreme warming trend continued, and again in 2016 (1.25 °C warmer than 1880–1909 conditions), a third year of record warmth, each year having surpassed the prior year, successively setting global temperature records. Then 2017, which was 1.16 °C above 1880–1909 norms, was the warmest non-El Niño year on record (UK Met Office, 2018). The coincidence of methane growth with these extreme years raises the question of the extent to which changes in temperature and precipitation may be contributing to the sustained growth rate in methane. This question is important because this type of climate system feedback effect is not explicitly parameterized in coupled atmosphere-ocean general circulation models. The temperature dependence of microbial methane emissions (Gedney et al., 2004; McNorton, Gloor, et al., 2016; Westerman & Ahring, 1987) suggests growth came as a response to that warmth. The very strong methane growth in 2014 may thus reflect the very warm temperatures compared to previous years.

Tropical wetland emissions respond quickly to warmth and increased precipitation and are relatively depleted in ^{13}C compared to the atmosphere (Brownlow et al., 2017; Dlugokencky et al., 2011; Nisbet et al., 2016). Flooding can be significant in expanding the surface area and hence emissions of key tropical wetlands. Mass transfer of water from ocean to land was tracked by the Gravity Recovery and Climate Experiment satellite (Boening et al., 2012). Analyzing Gravity Recovery and Climate Experiment data, Parker et al. (2018) found large discrepancies between estimates of CH_4 emissions based on GOSAT observations, and also emission estimates from land surface models, which may have badly underestimated tropical wetland methane emissions, by tens of teragrams.

Flooding may partly explain global methane growth in 2014–2018. Intuitively, warmer and wetter conditions would increase wetland emissions. Methane emission depends logarithmically on temperature and linearly on inundation areas. The very extensive wetlands in Bolivia had extreme flood events in early 2014 (Ovando et al., 2015), filling wetlands before the onset of intense heat in 2014. Growth in 2015 took place

in the powerful 2015–2016 El Niño, one of the strongest on record (L'Heureux et al., 2017; WMO, 2016). There were major rainfall anomalies, with increased rainfall in equatorial Africa and Angola/W.Zambia, as well as Paraguay, but drought in Amazonia (L'Heureux et al., 2017). Thus, the wetland record is complex. However, both Amazonia and tropical Africa, and indeed most of the planet, were extremely warm (L'Heureux et al., 2017). Thus, methane emissions may have grown as biogenic sources responded to both warmth and flooding. Similarly, 2016 was again a year of record warmth and the sustained methane rise in 2016, though not as strong as in the preceding 2 years, may also be primarily a biogenic response to the third successive increase in worldwide temperatures.

Ruminant emissions, especially cows, may also have played a major role (Schaefer et al., 2016; Wolf et al., 2017). Ruminant emissions are isotopically almost indistinguishable from wetland emissions. A cow is a walking wetland at 37 °C: methane from C4 (papyrus) equatorial wetlands and methane from cows fed with C4 fodder (maize, sugar cane waste) are isotopically similar and only distinguishable by back trajectory location and population analysis. Thus, it is probable that both wetlands and cows are contributing to current growth in tropical emissions. However, it should be noted that in India, the nation with by far the world's highest cattle population, atmospheric observations suggest there has been little or no growth in methane emissions between 2010 and 2015 (Ganesan et al., 2017). In other nations with very large ruminant populations (Brazil, China, United States, Ethiopia, Argentina, S. Sudan) this may not have been the case.

If the rise in methane and the simultaneous negative $\delta^{13}C_{CH4}$ shift have been driven by increased biogenic emissions, then it is feasible that an absolute increase in fossil fuel emissions may have coincided with a concurrent reduction in the fossil fuel proportion in the total methane emission source mix (Nisbet et al., 2016; Schaefer et al., 2016; Schwietzke et al., 2016). Methane emitted during extraction, transport, and combustion of coal and natural gas has characteristically more positive $\delta^{13}C_{CH4}$ (say −35‰ to −50‰) than the bulk −53‰ global methane source (Dlugokencky et al., 2011; Zazzeri et al., 2016), although it should be noted that the global mean for fossil fuel-related emissions has recently been shown to be around -44 ± 0.7‰, isotopically somewhat more negative than hitherto assumed (Schwietzke et al., 2017). Indeed, methane from some Arctic gas fields and also Australian coalfields has relatively negative $\delta^{13}C_{CH4}$ around −50‰ or less (Dlugokencky et al., 2011; Zazzeri et al., 2016), but these high latitude and southern emissions are geographically unlikely to have driven global methane growth, which has been led primarily from the wet tropics and low northern temperate latitudes.

The inference, that the share of global emissions coming from fossil fuels is dropping, sharply contradicts inventory evidence that global gas and coal production is growing (BP Statistical Review of World Energy, 2017, EDGAR, 2017) and that methane emissions from fossil fuels have risen substantially this century (EDGAR, 2017; USEPA, 2012). However, there is evidence (Schwietzke et al., 2016) that natural gas emissions per unit of production have declined significantly in recent years, and rapid improvements and investment in leak detection and reduction have likely cut the percentage of gas leaked from gas industry production facilities.

Observation of ethane trends (Hausmann et al., 2016) suggests growing emissions of methane from the hydrocarbon industry. Helmig et al. (2016) reported a recent increase in ethane emissions and that methane/ethane ratios could suggest that Northern Hemisphere oil and gas industry methane emissions had increased significantly recently (mid-2009 to mid-2014). But this assumes that ethane/methane ratios are constant and that they are coupled at large spatial scales: nevertheless, both assumptions can be challenged. Helmig et al. (2016) pointed out that such a postulated increase in gas emissions is inconsistent with observed leak rates and the isotopic results such as those cited above. Note also that ethane is released with methane in coal mining; thus, even if leaks have been reduced from natural gas facilities, the ethane record may reflect a growing contribution from coal mining, which has expanded greatly in East and South Asia in recent years.

Thus, although fossil fuel emissions of methane are very large and a more major part of the global budget than previously thought (Schwietzke et al., 2016), a simple explanation of the observed recent shift in $\delta^{13}C_{CH4}$ to values more depleted in ^{13}C, assuming the OH sink has been relatively unchanged, is that fossil emissions are falling as a proportion of the total methane emission (Nisbet et al., 2016; Schaefer et al., 2016), although they may have increased in absolute terms.

6.2. Has Either a Shift in Fossil Fuel $\delta^{13}C_{CH4}$ or a Decline in Biomass Burning Masked an Overall Increase in Fossil Fuel Emissions, While Sinks Remained Relatively Constant?

It is possible overall that methane emissions from fossil fuel sources have increased, but that the isotopic impact of this increase has been "masked" either because fossil fuel sources have overall become isotopically more negative, or because there has been a parallel decline in isotopically more positive output from biomass burning, or via some combination of both factors. This hypothesis assumes sinks have been steady.

Has the bulk $\delta^{13}C_{CH4}$ of global fossil fuel sources become more negative in the past decade? It is very difficult to comment on this, as measurements are inadequate. But the marked global trend away from coal and toward natural gas might support the notion. Methane from coal mines is isotopically variable: Zazzeri et al. (2016) suggested $\delta^{13}C_{CH4}$ values for bituminous coals of −65‰ for open cast mines and −55‰ for deep mines, while methane from anthracite mines ranged from −40‰ to −30‰. Thus, growth in open cast mines and closure of deep mines would shift the bulk $\delta^{13}C_{CH4}$ of emissions to more negative values. However, $\delta^{13}C_{CH4}$ shifts driven by changing methane fluxes from coal mines may have been counteracted by the rapid growth in extraction of natural gas. Schwietzke et al. (2016) have discussed these questions in detail.

A parallel contributory hypothesis is that a decline in biomass burning emissions has masked a strong increase in fossil fuel emissions, given evidence suggesting reduced burning in the 2001–2014 period (Worden et al., 2017). As noted above, Thompson et al. (2018) also infer that fossil fuel sources increased in 2006–2014, while biomass burning decreased. Methane from fires, especially in tropical savannas dominated by C4 grasses, is much enriched in $\delta^{13}C_{CH4}$ (Brownlow et al., 2017; Dlugokencky et al., 2011); thus, pulses of methane from tropical savanna and peatland fires ($\delta^{13}C_{CH4}$ around −30‰ to −15‰) have strong leverage on ambient values. If so, declines of emissions from smaller but more heavily $\delta^{13}C_{CH4}$ positive sources such as biomass burning (especially of tropical C4 grasses) and deep coal mining could have masked the isotopic impact of strong growth in emissions from industrial natural gas extraction, transmission, and use. Thus, a strong increase in emissions from natural gas leaks could indeed have occurred, as would be inferred from production growth (BP Statistical Review of World Energy, 2017), but with the isotopic impact hidden by the parallel decline in methane from fires. However, in this context it should be noted that there is evidence for doubling of ammonia emissions from biomass burning in the 2015 El Niño in S.E. Asia (Whitburn et al., 2016). Possibly the apparent standstill in the tropical $\delta^{13}C_{CH4}$ trend in the years 2014–2016 (see section 4.3) may reflect increased biomass burning methane emissions in this period.

What is clear is that because the $\delta^{13}C_{CH4}$ signature of biomass burning is relatively so positive, the global negative isotopic shift excludes an increase in biomass burning as an explanation for the methane rise, despite the warmth of 2015–2017, and this is supported by direct measurements of fire extent (van der Werf et al., 2017). Burnt area is not necessarily an accurate guide to methane emission from fires: the volume of the fuel load is arguably more important, especially in African grasslands. Carbon monoxide is another proxy for biomass burning, and has been broadly stable or declining at Ascension (NOAA data) and Zeppelin (NILU data). Much of this CO decline is in part as a result of controls on vehicle emissions (Yin et al., 2015), but a decline in biomass burning emissions is nevertheless plausible. Although Lelieveld et al. (2016) and Nicely et al. (2018) concluded that global OH is insensitive to perturbations by natural or anthropogenic emission changes, falling CO may also affect ratio of CO to NO_x regionally, and hence OH and the lifetime of methane in that region (see below).

Currently the data are inadequate to reach firm conclusions on these hypotheses. The more general inference is that the observed negative shift in $\delta^{13}C_{CH4}$ is not necessarily incompatible with an increase in overall fossil fuel emissions, if this increase has coincided with a shift from coal to gas, and/or a synchronous strong increase in emissions from sources with more negative $\delta^{13}C_{CH4}$ such as wetlands, and/or a decrease in a more positive $\delta^{13}C_{CH4}$ emissions, such as from biomass burning, or all factors together.

6.3. Possible Methane Sink Strength and Lifetime Changes Driven by a Decline in the Oxidative Capacity of the Atmosphere

An alternative explanation for the methane rise is that sinks have declined and thus methane's lifetime has increased, so that a given source supports a larger burden in the atmosphere. A decline in oxidation would lead to a negative $\delta^{13}C_{CH4}$ shift of the global methane burden. This would mean that methane's lifetime has increased such that a steady emission flux supports a higher atmospheric burden. Note that

the various hypotheses are nonexclusive: this could be a complementary hypothesis, concurrent with a change in sources.

Using a multispecies nonlinear Bayesian two-box inversion model to fit a smoothed deseasonalized hemispheric methane record, Turner et al. (2017) found that the most likely explanation for renewed growth in atmospheric methane was a 25 Tg/year decrease in total annual global methane emissions from 2003 to 2016, which was offset by a 7% decrease in global mean hydroxyl (OH) concentrations. However, this contrasts with the findings of Montzka et al. (2011) and Lelieveld et al. (2016) that OH is buffered and Dalsøren et al. (2016) who found increasing OH from 2003 to 2005 and stable OH during 2006–2012. As shown below, a decrease in the more highly fractionating removal by Cl could also explain much of the observed changes in methane mole fraction and $\delta^{13}C_{CH4}$, but it has to be a very large relative change in Cl together with some change in OH as well.

Rigby et al. (2017) also used a Bayesian study to model CH_3CCl_3 emissions as a proxy for OH and explore the methane growth up to 2014. They found that the likeliest explanation of the growth was that OH abundance grew by around 10% between the late 1990s and mid-2000s, and then fell by a similar magnitude from the mid-2000s to 2014. This is consistent with results from an ensemble of biogeochemical models (Poulter et al., 2017) that suggested the methane rise up to 2012 involved decreased tropical emissions. This would support explanations of growth that involved a combination of increasing fossil fuel and agriculture-related methane emissions and a decrease in the atmospheric oxidative sink.

Both studies (Rigby et al., 2017; Turner et al., 2017) commented that the problem is underdetermined: the long-term time series measurements of methane and $\delta^{13}C_{CH4}$ are inadequate, as is the knowledge of the regional variability of isotopic signatures of emissions from specific sources. Although not favored by their interpretations, neither Turner et al. (2017) nor Rigby et al. (2017) could discard the null hypothesis that OH has remained steady in recent years. Neither suggested any mechanism for the postulated changes in OH, although Dalsøren et al. (2016) point to the impact on OH of variations in NO_x, especially noting large increases in OH over Southeast Asia, mainly due to strong growth in NO_x emissions; more generally they commented that an increase in NO_x increases global OH as long as it takes place outside highly polluted regions.

These studies by Turner et al. (2017) and Rigby et al. (2017) raise the important question of what is happening to OH, the major methane sink. There is evidence for relatively small interannual variation (Montzka et al., 2011), although in some years changes >4% may have occurred. Yet the inversion models of Turner et al. (2017) and Rigby et al. (2017) suggest it fluctuates very much more. In contrast, Naus et al. (2019), using output from 3-D model simulations, found only small differences up to 1.3%, averaged over 1994–2015, in OH anomalies relative to the full uncertainty envelope (5–8%). The question is important not only for understanding the methane budget but also because the implications of any postulated substantial declines in the oxidative capacity of the atmosphere are profoundly worrying—the troubling inference is that the air is losing some of its self-cleansing mechanism. Discussing this debate, Prather and Holmes (2017) pointed to the need to push the box modeling nearer to the real world, to try to understand how climate changes or human actions can alter methane emissions and OH trends.

In both modeling studies, the main indicator species used for OH is methyl chloroform, CH_3CCl_3, but there are major problems in using this proxy. Although manufacture of this Montreal-Protocol species is formally prohibited, it is an excellent industrial solvent (e.g., for typing correction fluid), and thus there may be emissions continuing from landfills, especially in developing countries (Talaiekhozani et al., 2016). As possible parallels, Montzka et al. (2018) report an unexpected and persistent ongoing increase in prohibited CFC-11 emission and Vollmer et al. (2018) come to similar conclusions for ongoing CFC-13 output, possibly from East Asia. Until ongoing CH_3CCl_3 emissions are better quantified, or a new proxy for OH is found, our knowledge of OH and thus the oxidative capacity of the atmosphere will remain very poorly constrained. In this context, NIWA-New Zealand's ^{14}CO data that should be published shortly may provide a better proxy.

Dalsøren et al. (2016) investigated various factors influencing OH and found the ratio NO_x/CO is the most important. Until recently this ratio has increased, but new inventories from the Community Emission Data System (CEDS; Hoesly et al., 2017) indicate reduction in NO_x emissions and stable CO emissions.

This suggests a reduction in OH over the last few years, but data are inadequate to test the suggestion robustly. There are reasons to expect OH to be increasing in some places and decreasing in others (Dalsøren et al., 2016; Lelieveld et al., 2004, 2016), which could keep the global average constant with little effect on methane, but still have significantly different effects on short-lived trace gases depending on the spatial distributions and seasonality of their sources.

In this context, Thompson et al. (2018) found that OH appears not to have contributed significantly to recent methane growth. Further insight into the OH problem came from Nicely et al. (2018) who showed that atmospheric OH is probably currently well buffered, with mean anomalies of 1.6%. Although OH would be expected to decrease as methane rises, this effect is countered by the tropical widening as the Hadley cells expand (R. J. Allen et al., 2014), combined with the influences of changing H_2O, NO_x, and overhead O_3.

The timing of the isotopic shift provides a separate test of the "declining OH sink" hypothesis to explain the rise in methane. Methane destruction by OH changes the $\delta^{13}C_{CH4}$ value of the methane burden only slowly, over many decades (Tans, 1997), and interhemispheric $\delta^{13}C_{CH4}$ equilibration is slow. Methane's large seasonal cycles in emissions and removal mean that $\delta^{13}C_{CH4}$ never reaches equilibrium. Moreover, the seasonal cycles of mole fraction and $\delta^{13}C_{CH4}$ may be different, and perturbation impacts on $\delta^{13}C_{CH4}$ are sensitive to the time of year.

In contrast to the slow time scale of isotopic adjustment to changes in OH destruction, the "emission-driven" explanation of the methane rise, that pulses of emission inputs from biogenic sources took place, immediately changes regional and hemispheric $\delta^{13}C_{CH4}$. Imagine a major burst of wetland methane at the end of a wet season: this would cause regional $\delta^{13}C_{CH4}$ to plummet. This is exactly the type of rapid shift observed in the isotopic records illustrated in Figure 2. Sharp drops and peaks in $\delta^{13}C_{CH4}$ are visible, superimposed on the seasonality. These shifts are visible in multiple sites and are thus not just caused by local one-off meteorological variability. Such shifts are recorded (e.g., in 2014) by the coherent drops shown by the whole cortège of hemispheric stations, even in extratropical stations such as South Pole (Figure 2) and Cape Point (South Africa; see also Nisbet et al., 2016), which sample air masses far away from any local sources.

Given the slow time scale of $\delta^{13}C_{CH4}$ equilibration (Tans, 1997) it is hard to escape the inference that these shifts are too rapid to be solely a response to OH variation through the long-term kinetic isotopic impacts of OH destruction. More likely, the very rapid isotopic shifts in the record are driven, at least in part, by regional or hemispherical-scale source inputs. By fitting smoothed and deseasonalized curves to the measurement data, especially when using 1-box or 2-box models, inverse models can find apparent OH-led solutions for smoothed very long-term trends, but the very act of data smoothing raises the question whether critical emission-related insights from shorter-term variation are being lost.

Many of the possible changes in methane sources and/or sinks are direct or indirect responses to meteorological change. Wetlands may be warming, tropical ruminants may be flourishing more under better rainfall, or OH may be responding to change in the tropical troposphere. The negative shift in $\delta^{13}C_{CH4}$ suggests climate-linked processes are the most plausible explanations of the isotopic shift. Such decadal-scale feedbacks, especially in the tropics, may be secondary, not primary, anthropogenic forcings. The hypotheses that invoke primary anthropogenic inputs are the possibility that emissions from ruminants (primarily cattle) have increased, that a decline in biomass burning has masked the isotopic consequences of an increase in fossil fuel leaks, or that anthropogenic pollution may have caused OH decline.

7. Running Budget Model

To address the causes of methane growth, "running budget" modeling of data from 1998 to 2018 was carried out, extending the methodology developed by MRM in Nisbet et al. (2016) and summarized here in the supporting information. The previous analysis (Nisbet et al., 2016) investigated whether observed changes in methane mole fraction and isotopic content, averaged over four semihemispheric regions, could be explained by either of two end-member hypotheses: "increases in sources" or "declines in sinks." Optimization of fits to the observed seasonal cycles and trends in atmospheric data, by adjusting interannual changes in sources or sinks, has now been extended to use a significant revision of the highly isotopic fractionating removal of CH_4 by Cl (Hossaini et al., 2016), a more detailed treatment of the soil sink (Curry,

2007), and to include the more recent atmospheric data. Our analysis of semihemispheric source budgets is deliberately using a coarser resolution than is done in inverse models.

As noted above, Turner et al. (2017) considered that the most likely explanation of recent methane growth was that OH had declined, and Rigby et al. (2017) also found it very likely that an OH decline had played a major role in methane growth, while Naus et al. (2019) found that OH variation was likely to have been less. In contrast to Turner et al.'s (2017) modeling of smoothed multiyear trends, the inclusion of seasonal cycles in the analysis makes a significant difference when $\delta^{13}C_{CH4}$ data are considered. Neither CH_4 nor $\delta^{13}C_{CH4}$ are in equilibrium, and the two parameters have quite different response rates to budget changes (Tans, 1997), being nonlinear for $\delta^{13}C_{CH4}$. Thus, smoothing the record removes important signals. Nisbet et al. (2016) showed that a decrease in OH could indeed explain a shift in trend from $\delta^{13}C_{CH4}$ growing more positive to $\delta^{13}C_{CH4}$ growing more negative. But that explanation required a very significant change in OH and the slow timing of OH's effect on $\delta^{13}C_{CH4}$ meant that the sink hypothesis could not explain the large and rapidly occurring interannual variations observed in $\delta^{13}C_{CH4}$.

The analysis in Nisbet et al. (2016) suggested that for variation in the OH sink alone to be large enough to match the atmospheric data, significant changes in atmospheric chemistry would be seen in CO and non-methane hydrocarbons. However, that analysis did not consider trends and interannual variations in soil methanotrophy or in Cl removal, each of which have large isotopic fractionation effects: the extent that methane removal by Cl and soil methanotrophy can have impact on $\delta^{13}C_{CH4}$ fluctuations has not been considered hitherto. But, the recent increase in atmospheric methane would require total removal rates to have decreased by about 8%, which is close to the total removal by Cl and soil, thus the "Cl and soil" explanation would still require some decrease in OH as well. That possibility has been considered here by keeping sources constant after 2002 and fitting the data with annual changes in each of OH, Cl, and soil removal in each region. A tighter constraint is applied for OH than for the other removal processes.

In the analysis here, interannual changes in the methane budget start in 1998 when $\delta^{13}C_{CH4}$ data have global coverage. This comes after a "spin-up" period of more than 40 years to allow for the slow response of $\delta^{13}C_{CH4}$ to budget changes (Tans, 1997), and initialization of sources is made consistent with Lassey et al. (2007). Seasonal cycles for emissions and for their $\delta^{13}C$ signatures are fitted to the data in each region but do not change over time. The dominant methane removal by OH is from Spivakovsky et al. (2000) and the highly fractionating removal by Cl is using the "FULL2" seasonal and zonal distribution from Hossaini et al. (2016), which is predominantly in the Northern Hemisphere and so quite different to that of Allan et al. (2007), used in Nisbet et al. (2016). The seasonal and zonal distribution for soil removal of methane and its fractionation effect are from Curry (2007) and Tyler et al. (2007); methane removal by exchange with the stratosphere is treated as removal in the low latitudes with an implicit source in the high latitudes consistent with Brewer Dobson circulation. Exchange between the four tropospheric regions is allowed to vary annually after 1998 but is kept consistent with an interhemispheric exchange rate of 1–1.2 years as used in other studies.

Total methane removal is consistent with the last IPCC assessment (Ciais et al., 2013), except that the new and more detailed treatment of Cl removal is half of what was given there. The methane budget derived for each region is summarized in Table 1 which shows the source analysis for the 2000–2005 period. The total sources estimated here and their attribution into four regions is sensitive to our use of the Spivakovsky et al. (2000) distribution for OH but, as that is well backed up by other studies, the budgets can be given at least a medium confidence level. Note that the relatively large amount of Cl removal in the 30–90°N given by Hossaini et al. (2016) makes the sources there significantly isotopically lighter than in the other regions.

Fits to the mole fraction and $\delta^{13}C_{CH4}$ data are shown in Figure 4 and the corresponding source emissions and their $\delta^{13}C_{SRC}$ in Figure 5. Figure S1 shows that the fitting process does follow seasonal cycles in the data, but running 12-month means are used here to make differences between the fits clearer.

Because of different seasonal cycles and fractionation effects for each removal process, the net fractionation also has a significant seasonal cycle and differs between the semihemispheres. The budget totals fall between the top-down and bottom-up budgets given in the Ciais et al. (2013) review for the last IPCC Working Group I report. The lower parts of Table 1 summarize the *changes in source emissions* or *changes in removal* rates required after 2006 to follow the more recent mole fraction and $\delta^{13}C_{CH4}$ data and these are shown in Figure 5.

Table 1
Average Methane Removal Rates and Source Emissions Derived in This Analysis and Changes

	30–90°S	0–30°S	0–30°N	30–90°N	Global
OH lifetime (year)	18.6	6.8	7.1	15.0	9.8
Cl lifetime (year)	1,445	763	281	182	361
Soil lifetime (year)	655	132	165	125	173
Mean lifetime (year)	17.9	5.7	5.9	12.5	8.3
Mean KIE (‰)	−5.4	−4.7	−5.3	−12.3	−6.2
Mean source over 2000–2005					
Tg/year	62 ± 2	173 ± 4	198 ± 4	161 ± 4	594 ± 2
Annual cycle (Tg/year)	47	31–	165	270	378
Mean $\delta^{13}C$ (‰)	−51.8 ± 0.4	−52.0 ± 0.2	−51.9 ± 0.2	−56.3 ± 0.2	−53.1 ± 0.2
Annual cycle $\delta^{13}C$ (‰)	8.7	2.7	7.3	13.8	7.8
Changes in sources					
2007–2014 relative to 2000–2005					
Tg/year	+4.8 ± 1	+4.9 ± 2	11.7 ± 2	5.0 ± 2	26.4 ± 2
$\delta^{13}C$ (‰)	−0.7 ± 0.2	−0.2 ± 0.1	+0.2 ± 0.1	−0.4 ± 0.1	−0.2 ± 0.1
2015–2018 relative to 2000–2005					
Tg/year	+7.7 ± 1	+12.4 ± 3	+17.6 ± 3	+6.3 ± 2	+43.8 ± 2
$\delta^{13}C$ (‰)	−0.5 ± 0.2	−0.2 ± 0.2	−0.1 ± 0.2	−0.7 ± 0.1	−0.3 ± 0.2
Changes in removal					
2007–2014 relative to 2000–2005					
Tg/year	−3.2 ± 0.6	−2.7 ± 1.1	−10.2 ± 1.2	−3.5 ± 1.2	−19.6 ± 2.1
Change in KIE (‰)	+0.3 ± 0.1	+0.2 ± 0.1	−0.1 ± 0.1	+0.40 ± 0.3	+0.2 ± 0.1
2015–2018 relative to 2000–2005					
Tg/year	−5.7 ± 0.5	−12.9 ± 0.7	−15.8 ± 1.0	−7.5 ± 0.6	−41.7 ± 1.5
Change in KIE (‰)	+0.3 ± 0.1	+0.2 ± 0.1	0 ± 0.1	+1.4 ± 0.2	+0.5 ± 0.1

Note. The upper two parts of the table summarize lifetimes and then sources with their $\delta^{13}C_{CH4}$ values, averaged over the 2000–2005 period, that match the observed mole fraction and $\delta^{13}C_{CH4}$ data. Mean lifetimes include cross-tropopause transport followed by removal in the stratosphere consistent with Ciais et al. (2013). Larger emission uncertainties in most regions than in the global total reflect the uncertainties in exchange rates between the semihemispheres. The lower parts summarize changes in emissions and their $\delta^{13}C_{CH4}$, or in the removal rate and its kinetic isotope effect, that match data over 2007–2014 and then 2015–2018.

Fitting changes in source emissions, as shown in Figure 5, leads to global emissions increasing significantly in 2006 and again in 2013 and by about 20 Tg/year in each case, but significant interannual variability is also seen in the semihemispheres. Sources have been getting isotopically lighter in 30–90°N and 0–30°S but not in 0–30°N. Note that relatively small emission in the 30–90°S zone makes it much more sensitive to interannual variations in transport, so the negative trend there is not robust. Anticorrelations between source emissions in 0–30°N and in 30–90°N such as seen over 2012–2018 also suggest that this simple budget analysis may not cover variations in the transport between regions.

Fits to the data with changes in removal rate, and sources constant after 2002, are also shown in Figure 5 (with more details in Figures S1 and S2). These have constraints on OH of ±5% and on Cl and soil removal of ±20%. As shown in Figure S1, these fits have removal rates starting near the high end of their allowed range over 2000–2005, dropping to an intermediate level in 2006, and then close to their lowest allowed level in 2013. This corresponds to transitions between three average removal rates corresponding to mean CH_4 lifetimes of 7.9, 8.3, and 8.6 years and, as shown in Figure 5, decreases in CH_4 removal are similar to optimized increases in emission when removal rates are fixed. Results from restricting OH changes to ±2% are shown in Figures 4 and 5 and do not follow either mole fraction or $\delta^{13}C_{CH4}$ very well, while allowing OH changes of ±10% made very little difference from ±5%. When only OH is allowed to change, the fit to mole fraction is plausible, that for the $\delta^{13}C_{CH4}$ data is much worse.

Independent annual changes in removal for each of the four regions and for each of the OH, Cl, and soil processes are highly variable as shown (Figure S2) implying that these are not well determined by the CH_4 data. Also, while large relative changes in Cl and soil removal together with smaller ones for OH can follow much of the trends and variability in mole fraction and $\delta^{13}C_{CH4}$, large variations such as seen in the mole fraction in 2003 and in the $\delta^{13}C_{CH4}$ in 2008 are better reproduced by variations in sources.

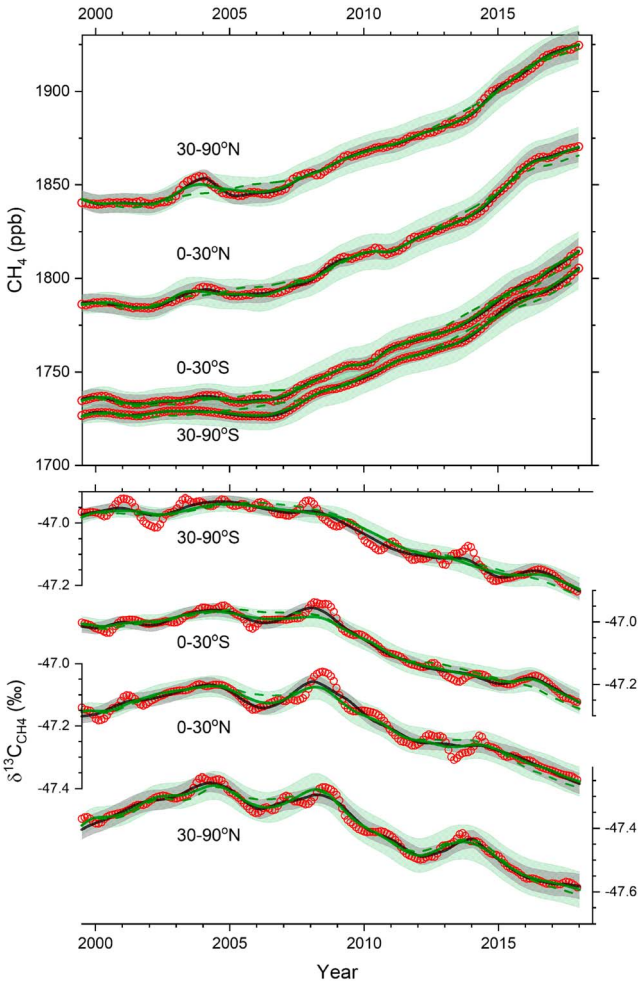

Figure 4. Running 12-month means for the CH_4 mole fraction and $\delta^{13}C_{CH4}$ (red open circles) data are shown averaged over the four regions using data to mid-2018. Fits to the data are shown for "changes in source emissions" (black line and gray uncertainty range). Similar fits for "changes in removal" rate that have reduction in OH limited to 5% and in Cl and soil removal to 20% are also shown (green lines and pale green uncertainty range). For comparison, dashed green lines show the results when OH variations are limited to 2%.

Figure 4 shows that fits to the mole fraction and $\delta^{13}C_{CH4}$ data using changes in removal rates match the alternative explanation of changes in source emissions quite closely when large interannual changes in Cl and soil removal are used with smaller ones for OH. However, large variations such as seen in the mole fraction in 2003 and in the $\delta^{13}C_{CH4}$ in 2008 are better reproduced by *changes in sources*. But this does not mean that removal rates have been constant. Rather, it shows that the problem is underdetermined and that interannual fluctuations in soil methanotrophy and the Cl sink could still be relevant, particularly in explaining some —but very unlikely, all—of the variations observed.

Answering the "sources versus sinks" debate clearly requires more isotopic data, especially in the tropics: to close the budget the enormous data gap in the tropical and subtropical regions needs to be filled. In particular, $\delta^{13}C_{CH4}$ is currently only measured at a very small number of stations. Ambiguities in the $\delta^{13}C_{CH4}$ budget analysis could be reduced by more extensive use of methane's other isotopic parameters. In particular, long-term time series of δD_{CH4} would provide powerful constraints on the problem, but currently data are minimal and there are very few active long-term measurement sites. Multiple substituted or "clumped" isotopologues in methane also carry powerful information (Stolper et al., 2015) but this is frontier work only just beginning. Finding a good proxy for OH concentration in the atmosphere, and also determining the size of ongoing CH_3CCl_3 emission is urgent.

A common factor linking many of the plausible explanations of the methane increase and isotopic shift since 2007—whether growth in biogenic emissions, or sink declines—is that they may result from possible feedbacks to meteorological change that are not included in most current climate models: the study by Naus et al. (2019) demonstrates the need for a proper modeling framework. The high growth in the Arctic in 2007, the global 2007–2009 growth, the impact of the 2010 La Niña in the tropics, and the 4 years of growth in 2014–2017 all suggest powerful feedbacks between the extreme meteorology of these years and methane growth.

8. Constraints on the Paris Agreement Target, Given Methane's Growth

The methane rise has already had direct impact on the 2015 Paris Agreement, under which the UN Framework Convention on Climate Change (UNFCCC) set a goal of constraining future climate warming to a 2 °C rise (UNFCCC, 2015, 2017). Achievement of this ambitious warming outcome requires keeping the maximum anthropogenic radiative forcing to around 3 W/m^2 (Meinshausen et al., 2011; Rogelj et al., 2012; see also IPCC, 2018). This very challenging target demands rapid and severe cuts on anthropogenic greenhouse gas emissions, supported by an active program to monitor, quantify, and control or remove them. The abatement potential of non-CO_2 reduction has a major impact on the allowable cumulative CO_2 emission and cumulative abatement costs (Rogelj et al., 2015). In particular, to attain a sharp near-future reduction in radiative forcing by atmospheric greenhouse gases, the methane burden needs to be cut very rapidly indeed (Meinshausen et al., 2011; Rogelj et al., 2012).

The IPCC Summary for Policymakers on Global Warming of 1.5 °C (IPCC, 2018) updates the earlier Paris Agreement pathways, emphasizing the importance of constraining global climate warming below a 1.5 °C limit. This report highlights the major role that can be played by reductions in methane. Given sharp cuts in the atmospheric methane burden (as well as black carbon and N_2O), coupled with strong reductions in CO_2 emissions and carbon removal by forest regrowth, then it may yet be possible to attain the 1.5 °C goal. However, if non-CO_2 emissions are not cut, then the only way of meeting the 1.5 °C target is with heroic

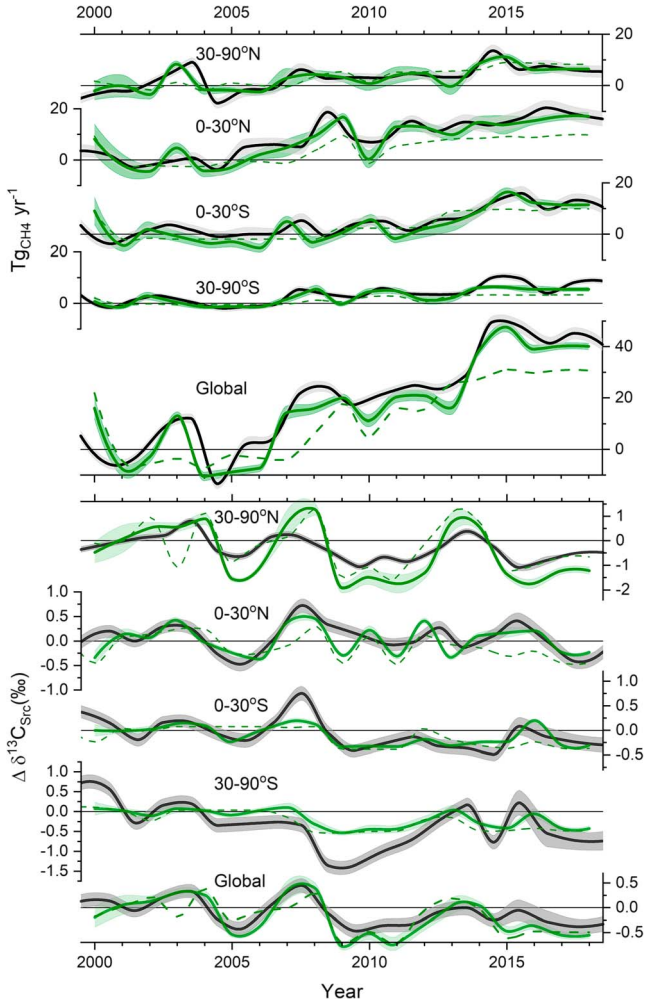

Figure 5. The upper panel shows interannual "changes in sources" fitted to the data for each region and the global average (black with gray uncertainty range) relative to 2000–2005. The alternative for "changes in removal" fitted to the data are also shown (green with pale green uncertainty range). Again, dashed green lines show results when OH variations are limited to 2%. The lower panel shows the changes in each region's source $\delta^{13}C$ value and the global average (black with gray uncertainty range) as well as changes in the net kinetic isotope effect (green with pale green uncertainty range) due to relative changes in the role of OH, Cl, and soil.

industrial-scale CO_2 removal in addition to reforestation. The evidence for methane growth presented here raises the possibility that should methane's current rate of increase continue for some decades, the Paris target may become intractable to attain.

Representative Concentration Pathway 2.6 (RCP2.6; Moss et al., 2008; Meinshausen et al., 2011; van Vuuren et al., 2011; here defined as updated by M. Collins et al., 2013) is a standard emission scenario pathway that is capable of taking us to the Paris goal (Rogelj et al., 2012). RCP2.6 (Meinshausen et al., 2011; Moss et al., 2008; van Vuuren et al., 2011), defined as updated by M. Collins et al. (2013), can, if followed, achieve a Paris-compliant target, leading to likely peak warming between 1.2 and 2.0 °C (Millar et al., 2017). But the RCP2.6 pathway is extremely demanding; moreover, there are uncertainties over the extent of current warming (Cowtan et al., 2015; Schurer et al., 2018) and about the definition of the target (Hawkins et al., 2017).

A key contribution built into the RCP2.6 pathway is a 500 ppb reduction in methane this century, from 1754 ppb (taken as the baseline value in 2005) dropping after 2010 by about 6 ppb per year to 1,452 ppb in 2050, then dropping by about 4 ppb a year to 1,254 ppb in 2100 (Meinshausen et al., 2011). This would cut the total atmospheric methane burden by about 1,400 Tg compared to the assumed baseline value, or by about 1,660 Tg compared to the methane burden in 2018. To achieve this reduction would demand a cut in annual emissions of roughly 150 Tg during this century (2.77 Tg of CH_4, distributed evenly into the global atmosphere, will increase the global mole fraction by 1 ppb).

But the methane burden is not dropping. The opposite is happening. By mid-2018, we were already >100 ppb above the methane projection used in RCP2.6 (Figure 6). If present growth rates are sustained to 2100, this would add another 600 ppb, taking methane to around 2,400 ppb or nearly double the Paris-compliant IPCC RCP2.6 scenario. Even if methane growth only continued to 2050, the impact on compliance with Paris Agreement expectations would be severe. Figure 6 shows the discrepancy in warming impact (mW/m^2) that has already opened up between the "Paris-compliant" RCP2.6 and the present (end-2017) methane burden. The methane increase since 2007 has given a radiative forcing of 0.05 W/m^2 for methane compared to RCP2.6. If this continues another 10 years it would be a radiative forcing of about 0.1 W/m^2. That would be of the same order as the current increase in current CO_2 radiative forcing over 3 years.

There is a further troubling factor, not appreciated at the time the Paris Agreement was negotiated. Recent reevaluation of the radiative forcing from methane (W. D. Collins et al., 2018; Etminan et al., 2016), including shortwave radiation effects, has found the forcing of methane since preindustrial times to be about 25% stronger than the value used in the IPCC (Stocker et al., 2013) assessment. This reevaluates methane's 100-year global warming potential (GWP_{100}) factor as 32, or 14% higher than previously thought, though it should be noted that this value is provisional. GWP_{100} is a measure of the integrated radiative forcing from equal-mass pulsed emission of a gas relative to CO_2 and is used to determine trade-offs between different gases, evaluated over a 100-year time scale. It is commonly used to determine how much CO_2 should be removed to compensate for methane emissions. But the evolving value for GWP_{100} demonstrates the problems with using it to evaluate equivalences between different greenhouse gases. For the Kyoto Protocol the UNFCCC used a value of 21 from the IPCC's second assessment report, published in 1996, and a GWP_{100} of 25 for the Doha Amendment covering 2013–2020 (http://unfccc.int/resource/docs/2013/cop19/eng/10a03.pdf).

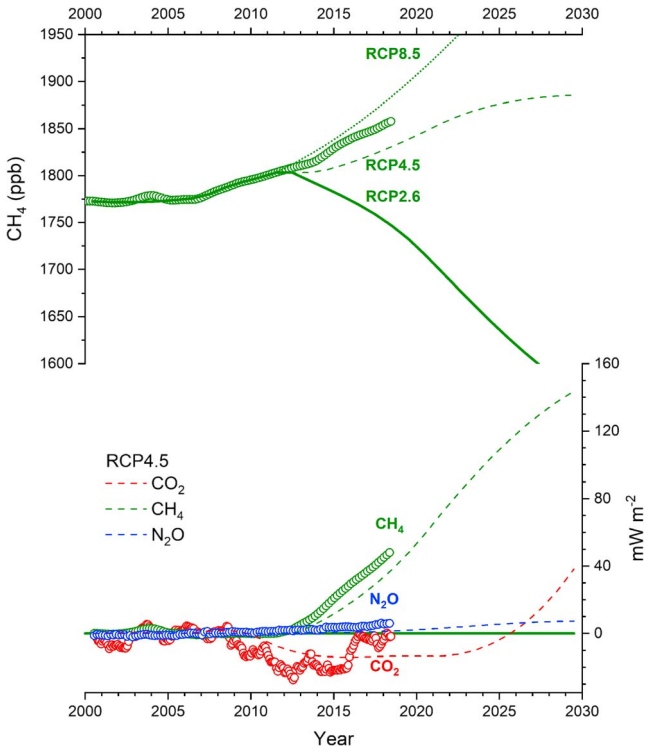

Figure 6. Top Panel: Observed global average methane (green open circles) at 3-monthly intervals (National Oceanic and Atmospheric Administration) are compared with the RCPs used in climate models (green solid, dashed, and dotted lines). Lower Panel shows differences in radiative forcing between actual evolution of methane (green open circles), CO_2 (red circles), and nitrous oxide (blue circles) compared to the RCP2.6 pathway (0 solid line) and corresponding differences for the RCP4.5 pathway (dashed lines). Actual radiative forcing, 2000-present (shown as solid lines), from key gases in milliWatts per square meter expressed as deviation from the RCP2.6 IPCC AR5 pathway (0 line on graph), which is compliant with the Paris target (Meinshausen et al., 2011; Rogelj et al., 2012). RCPs from IPCC AR5 Working Group 1 Appendix (M. Collins et al., 2013). For further context, the RCP4.5 scenario is also shown, to 2030 (dashed lines). For methane, current trends are higher even than the RCP4.5 scenario. Note that until the 2020s the RCP4.5 path does have lower CO_2 concentrations than the RCP2.6 path. RCP = Representative Concentration Pathway.

The relevance of GWP_{100} to the Paris Agreement has been discussed in recent papers (M. R. Allen et al., 2018; Fuglestvedt et al., 2018; Tanaka & O'Neill, 2018). CO_2-equivalent emissions of methane calculated using GWP_{100} do not predict the resultant warming, because methane does not remain in the atmosphere as long as CO_2. M. R. Allen et al. (2018) show that in scenarios that achieve the Paris Agreement goals, GWP_{100} misrepresents the impact of methane on temperature. They apply GWP_{100} to a sustained change in the emission rate of methane (instead of a pulse), introducing a new parameter (GWP*) to relate the impacts on radiative forcings of emissions of both short-lived and long-lived species. This method of relating CO_2-equivalent emissions that are equivalent in their temperature response may allow relative evaluation of mitigation initiatives for different greenhouse gases. In contrast to GWP_{100}, GWP* correctly links increasing methane emissions with the resultant atmosphere warming, and decreasing emissions with atmospheric cooling.

To summarize, in terms of radiative forcing, the methane growth in the past decade has added about 0.025 or 0.05 W/m^2 relative to the RCP2.6 expectation (Figure 6). At this growth rate, if sustained to 2100, methane would add more than 0.5 W/m^2 of unexpected forcing compared to the Paris target. Thus, even if anthropogenic CO_2 emissions are successfully constrained to a RCP2.6-like pathway, the unexpected and sustained current rise in methane may so greatly overwhelm all progress from other reduction efforts that the Paris Agreement will fail.

In the context of the UNFCCC it should be noted that the global methane emissions budget remains unconstrained (Kirschke et al., 2013; Saunois, Bousquet, et al., 2016; Saunois, Jackson, et al., 2016) and there is concern about so-called “bottom-up” inventory assessments, made by aggregating estimates of emissions from local, regional, and national statistics and databases, total 600–900 Tg/year. In sharp contrast, if OH is buffered, “top-down” budgets calculated by modeling measurements of the ambient atmosphere result in annual emissions between 560 and 580 Tg (Saunois, Bousquet, et al., 2016). One explanation of the discrepancy is that inventories may include double-counting of natural emissions (Thornton, Wik, et al., 2016). For the Paris Agreement to succeed and for reduction policies to be realistic, much better knowledge and much more accurate budgets are urgently required to bring bottom-up assessments into agreement with top-down measurements (Nisbet & Weiss, 2010).

9. Discussion

Speaking before the 2015 Paris Agreement, President Obama noted that in 2014 “the world economy grew while global carbon emissions from burning fossil fuels stayed flat. And what this means can't be overstated” (Obama, 2015). The Paris Agreement is ambitious, yet, as Obama pointed out, and despite the continuing very strong growth in the atmospheric burden of CO_2, there is optimism that reaching the target may just be feasible for CO_2 itself. But little attention was paid to the extraordinary rise in methane that year, despite methane's major contribution to the total anthropogenic warming to date. The Paris Agreement goals permit only a limited time to achieve net-zero CO_2 emissions before we overshoot the Agreement's warming limit. The more the atmospheric methane burden grows, the less time we have to reach net-zero CO_2 emissions.

The recent methane growth, and especially the acceleration in 2014, came as a surprise. If the processes driving growth are not directly anthropogenic, for example, tropical rainfall or OH, Cl, and soil sink changes, then the ~75 ppb scale of the recent rise so far is unprecedented in the Holocene record. For

comparison, for fluctuations in the late Holocene Rhodes et al. (2017) find variabilities of 10–40 ppb. As noted above, large uncertainties remain in the global methane budget, and top-down and bottom-up estimates have not yet been reconciled. There remain major uncertainties about the emissions contributed by fossil fuel, agricultural and natural sources, and the proportions they constitute in the total budget. Unless the reasons for the current rise are understood, and it is determined whether or not growth is due to climate change feedbacks, it will not be possible to predict future trends in methane, nor to manage future feedbacks that may be driving the increase. Interestingly, although there may be no common causal link, the methane growth since 2007 and accelerated growth since 2014, both parallel increases in another major indicator of climate change, the rates of ice loss from both the Arctic (NSIDC, 2018) and West Antarctica (IMBIE, 2018).

It is clear that if the Paris Agreement is to succeed, methane must be understood, but there are large unknowns. The key global deficiency, as noted by modeling studies (Rigby et al., 2017; Turner et al., 2017) is the lack of long-term measurement data from remote sites, especially in the tropics. There is urgent need for more in situ observations, from more locations, to constrain atmospheric inverse models of the methane budget. Isotopic measurement remains very sparse indeed. Satellite retrievals are unable to determine boundary layer methane abundance or to observe isotopologues accurately. To resolve the OH puzzle, more stations measuring long-term time series of methane mole fraction, $\delta^{13}C_{CH4}$ and δD_{CH4} are needed, especially in the tropics, as well as a tighter understanding of ongoing methyl chloroform (CH_3CCl_3) emissions. But funding agencies prioritize hypothesis-testing and process-study campaigns over long-term monitoring.

There is a further ground for concern. There are very serious global implications for air quality if the rise in methane is due to a sharp drop in the oxidative capacity—the cleansing power—of the atmosphere, as implied by Turner et al. (2017) and to some extent by Rigby et al. (2017) and Poulter et al. (2017). If so, there are wide-ranging implications for many fields of atmospheric science that go far beyond greenhouse gas budget studies. It is very important to test the hypothesis that the oxidative capacity of the air has declined.

There is urgent need to quantify the necessary reduction of methane emissions to meet Paris Agreement goals and to identify target sources for reduction. A key problem for the UNFCCC is the weakness of emissions inventories for methane sourced in so-called “non-Annex 1” countries. These are emerging economies and low-income “developing” nations, including China, India, Africa, and South America except French Guiana. These non-Annex 1 states include all tropical nations, including Singapore, Saudi Arabia, and Qatar. The only tropical areas with more rigorous constraints on their inventory reporting are tropical territories of the United States, Australia, France, and the United Kingdom. Quantifying and regularly updating emissions from low-income tropical nations is urgent, both bottom-up and top-down. But setting up new monitoring sites is difficult as equipment import regulations are typically prohibitive, local interest and support may be low, and access difficult.

For methane, this is a grave weakness. Tropical and subtropical emissions are critical in the global budget, both from anthropogenic sources including widely developing gasfields and some coalfields, the world's largest cattle populations and widespread deliberate biomass burning, and also from natural emissions in the very large wetlands of Amazonia and the Pantanal in South America, the Congo, Zambesi, and other major river basins in Africa, and in S.E. Asia. Methane emissions have high societal cost (Shindell et al., 2017).

In contrast to CO_2, methane provides many attractive, economically feasible, and socially acceptable targets in reducing national and global emissions relatively inexpensively. A very attractive option is to be more vigorous in reducing fossil fuel emissions from gas leaks and coal processing. Emissions from fossil fuels and natural geological sources may be a higher fraction of the total global methane budget than previously thought, and may have been 195 $\pm$ 32 Tg/year in the 2003–2013 decade (Schwietzke et al., 2016). This result compares with a value of about 30.0% of total emissions (circa 160–170 Tg) estimated from radiocarbon measurements (Lassey et al., 2007). Moreover, ice-core studies suggest that natural emissions from geological sources during the Younger Dryas were no higher than 15.4 Tg annually (Petrenko et al., 2017), much less than the >50 Tg/year currently estimated. If geological emissions have not markedly changed since glacial times, modern annual anthropogenic fossil fuel emissions are correspondingly greater by ~35 Tg/year.

There are many good targets for reduction of methane emissions from fossil fuels. Leakage rates remain very significant (Peischl et al., 2016; Zavala-Araiza et al., 2015). Recent U.S. evidence (Alvarez et al., 2018) suggests the gas leaks from the U.S. supply chain are around 2.3% of gross gas production, or about 13 ± 2 Tg/year, which is ~60% higher than U.S. EPA inventory estimate. Recently, there has been rapid progress in technical methods to detect anthropogenic methane sources and in assessing their emission fluxes (Peischl et al., 2016; Schwietzke et al., 2017; Zavala-Araiza et al., 2015; Zazzeri et al., 2016). The disproportionate role of super-emitters has been widely observed (e.g., Zavala-Araiza et al., 2015). In the Barnett Shale gasfield in Texas, half of methane emissions came from 2% of the oil and gas facilities at any one time (Zavala-Araiza et al., 2015). Similar patterns of super-emission from abandoned wells and coal-mine vents were also found in Queensland and New South Wales, Australia (Zazzeri et al., 2016). Detection and monitoring of super-emitters is rapidly becoming simpler with the rapid advances in vehicle-based sensors (e.g., Zazzeri et al., 2015), aircraft measurement (Schwietzke et al., 2017), and satellite sensing, and continuous monitoring is now feasible around production sites, to watch super-emitters and potential super-emitters across their life cycle. Thus, targeting super-emitters and working with operators to improve operational practices can enable rapid, low-cost cuts in emissions (Mayfield et al., 2017). Cutting gas leaks and landfill emissions, which is strongly supported by industry and the UN Climate and Clean Air Coalition (BP, 2018), should be a global priority.

There are large potential benefits in dietary change (e.g., Ritchie et al., 2018), especially reduction in intense factory farming of cattle, but the net cut in methane emission from taking pastureland out of food production is not easily quantified. Replacing organic beef from rocky Scottish hills with soya grown intensively on former tropical rainforest or cerrado is not necessarily advantageous. Moreover, forced reduction in cattle numbers is socially unacceptable in key regions: by far the largest population of ruminants is in India, while Ethiopia and South Sudan also have globally significant ruminant populations. Similarly, "mitigation" of wetland emissions has been suggested (e.g., Zhang et al., 2017). But such interventionist policies may not be feasible, could damage tropical wetlands with unpredictable consequences, and provoke strong local political antagonism to concerns about global warming.

There is more opportunity for cutting tropical biomass burning, which is easily observed and widely damaging agriculturally (exporting valuable soil nutrients to the wind). Reducing burning with targeted locally based community-reward schemes is feasible, inexpensive, and should have wide beneficial impact. Removal of methane from ambient air has had little attention, but initial work suggests it may be simple and inexpensive in certain settings.

We may not be able to influence the factors driving the new rise in methane, especially if it is a climate change feedback, but by monitoring, quantifying, and reducing the very large anthropogenic inputs, especially from the gas, coal, and cattle industries, and perhaps by direct removal, we may be able to cut the total methane burden to be compliant with the Paris goals.

10. Conclusion

The need to determine the factors behind the recent rise in methane is urgent: indeed, essential if global warming is to be limited within the Paris Agreement limits. If the main causes are increased anthropogenic emissions, they need to be reduced. If the increased methane burden is driven by increased emissions from natural sources, and if this is a climate feedback—the warming feeding the warming—then there is urgency to reduce anthropogenic emissions, which we can control. If, however, the increase in the methane burden is driven by a decline in the oxidative capacity of the atmosphere, and this is a climate feedback, then the implications are serious indeed.

Reducing methane emissions is feasible, especially from fossil fuel sources, and would have rapid impact on the global methane burden. This permits optimism but not complacency: the challenge is large. But there is no single silver bullet: there are many frontiers in methane research, and successfully meeting the Paris goals demands wide-ranging progress. Unless these questions are addressed, and much more attention paid to reducing methane emissions, especially from fossil fuels and biomass burning, the success of the Paris Agreement may be at risk.

Acknowledgments

We thank our many field site partners and measurement teams for sustained dedication in gathering multiyear data sets through the vagaries of funding. Their work is invaluable in understanding global greenhouse gas growth. The NOAA Cooperative Global Air Sampling Network underpins all study of the methane burden in the global atmosphere. The RHUL observations are particularly dependent on the painstaking measurement of Mathias Lanoisellé and Barbara White, and for sustained support from the UK Met Office in Ascension Is., from Environment and Climate Change Canada (D. Worthy and colleagues) and the South African Weather Service, who maintain the globally important site at Cape Point. We thank Kirk Thoning (NOAA) for helping prepare two figures. We thank Keith Shine, Rona Thompson, and the editor and anonymous referees for thoughtful, detailed, and very valuable criticism. NOAA data are available online (https://www.esrl.noaa.gov/gmd/dv/data/). RHUL data are being archived in the UK Centre for Environmental Data Analysis (CEDA; http://catalogue.ceda.ac.uk/uuid/dd2b03d085c5494a8cbfc6b4b99ca702). This work was supported by the UK Natural Environment Research Council's MOYA (Global Methane Budget) project; as well as by a sequence of prior projects supported by NERC (MAMM, Arctic methane, Southern methane) and the European Union (InGOS, Geomon, IMECC, Meth-MonitEUr, etc.) over the past 20 years; and also by the MOCA (Methane emissions from the Arctic Ocean) and SOCA (Signals from the Arctic OCean to the Atmosphere) projects, funded by the Research Council of Norway.

References

Allan, W., Struthers, H., & Lowe, D. C. (2007). Methane carbon isotope effects caused by atomic chlorine in the marine boundary layer: Global model results compared with Southern Hemisphere measurements. *Journal of Geophysical Research*, *112*, D04306. https://doi.org/10.1029/2006JD007369

Allen, M. R., Shine, K. P., Fuglestvedt, J. S., Millar, R. J., Cain, M., Frame, D. J., & Macey, A. H. (2018). A solution to the misrepresentations of CO2-equivalent emissions of short-lived climate pollutants under ambitious mitigation. *Npj Climate and Atmospheric Science*, *1*, 16. https://doi.org/10.1038/s41612-018-0026-8

Allen, R. J., Norris, J. R., & Kovilakam, M. (2014). Influence of anthropogenic aerosols and the Pacific Decadal Oscillation on tropical belt width. *Nature Geoscience*, *7*(4), 270–274. https://doi.org/10.1038/ngeo2091

Alvarez, R. A., Zavala-Araiza, D., Lyon, D. R., Allen, D. T., Barkley, Z. R., Brandt, A. R., et al. (2018). Assessment of methane emissions from the US oil and gas supply chain. *Science*, *361*, 186–188. https://doi.org/10.1126/science.aar7204(2018)

Berchet, A., Bousquet, P., Pison, I., Locatelli, R., Chevallier, F., Paris, J. D., et al. (2016). Atmospheric constraints on the methane emissions from the East Siberian Shelf. *Atmospheric Chemistry and Physics*, *16*, 4147–4157. https://doi.org/10.5194/acp-16-4147-2016

Boening, C., Willis, J. K., Landerer, F. W., & Nerem, R. S. (2012). The 2011 La Niña: So strong, the oceans fell. *Geophysical Research Letters*, *39*, L19602. https://doi.org/10.1029/2012GL053055

Bousquet, P., Ciais, P., Miller, J. B., Dlugokencky, E. J., Hauglustaine, D. A., Prigent, C., et al. (2006). Contribution of anthropogenic and natural sources to atmospheric methane variability. *Nature*, *443*, 439–443. https://doi.org/10.1038/nature05132

Bousquet, P., Ringeval, B., Pison, I., Dlugokencky, E. J., Brunke, E. G., Carouge, C., et al. (2011). Source attribution of the changes in atmospheric methane for 2006–2008. *Atmospheric Chemistry and Physics*, *11*, 3689–3700. https://doi.org/10.5194/acp-11-3689-2011

BP (2018). Methane matters. Retrieved from http://share.world-television.com/d/22906-Methane+Matters+Highlights+v12_H264_HI-RES.mp4

BP Statistical Review of World Energy (2017). Retrieved from http://www.bp.com/statisticalreview

Brownlow, R., Lowry, D., Fisher, R. E., France, J. L., Lanoisellé, M., White, B., et al. (2017). Isotopic ratios of tropical methane emissions by atmospheric measurement. *Global Biogeochemical Cycles*, *31*, 1408–1419. https://doi.org/10.1002/2017GB005689

Brownlow, R., Lowry, D., Thomas, R. M., Fisher, R. E., France, J. L., Cain, M., et al. (2016). Methane mole fraction and δ13C above and below the trade wind inversion at Ascension Island in air sampled by aerial robotics. *Geophysical Research Letters*, *43*, 11,893–11,902. https://doi.org/10.1002/2016GL071155

Cantrell, C. A., Shetter, R. E., McDaniel, A. H., Calvert, J. G., Davidson, J. A., Lowe, D. C., et al. (1990). Carbon kinetic isotope effect in the oxidation of methane by the hydroxyl radical. *Journal of Geophysical Research*, *95*(D13), 22,455–22,462. https://doi.org/10.1029/JD095iD13p22455

Ciais, P., Sabine, C., Bala, G., Bopp, L., Brovkin, V., & House, J. I. (2013). Carbon and other biogeochemical cycles. Chapter 6. In T. F. Stocker, et al. (Eds.), *Climate change 2013: The physical science basis. Contribution of working group I to the fifth assessment report of the intergovernmental panel on climate change* (pp. 465–570). Cambridge, UK and New York: Cambridge University Press.

Collins, M., Knutti, R., Arblaster, J., Dufresne, J. L., & Fichefet, T. (2013). Section 12.3.1.3 The new concentration driven RCP scenarios, and their extensions. In T. F. Stocker, et al. (Eds.), *Climate change 2013: The physical science basis. Contribution of working group I to the fifth assessment report of the intergovernmental panel on climate change* (pp. 1029–1136). Cambridge, UK and New York: Cambridge University Press.

Collins, W. D., Kuo, C., & Nguyen, N. H. (2018). Large regional shortwave forcing by anthropogenic methane informed by Jovian observations. *Science Advances*, *4*(9), eaas9593. https://doi.org/10.1126/sciadv.aas9593

Cowtan, K. Z., Hausfather, Z., Hawkins, E., Jacobs, P., Mann, M. E., Miller, S. K., et al. (2015). Robust comparison of climate models with observations using blended land air and ocean sea surface temperatures. *Geophysical Research Letters*, *42*, 6526–6534. https://doi.org/10.1002/2015GL064888

Crutzen, P. J., & Andreae, M. O. (1990). Biomass burning in the tropics: Impact on atmospheric chemistry and biogeochemical cycles. *Science*, *250*, 1669–1678. https://doi.org/10.1126/science.250.4988.1669

Curry, C. L. (2007). Modeling the soil consumption of atmospheric methane at the global scale. *Global Biogeochemical Cycles*, *21*, GB4012. https://doi.org/10.1029/2006GB002818

Dalsøren, S. B., Myhre, C. L., Myhre, G., Gomez-Pelaez, A. J., Søvde, O. A., Isaksen, I. S. A., et al. (2016). Atmospheric methane evolution the last 40 years. *Atmospheric Chemistry and Physics*, *16*, 3099–3126. https://doi.org/10.5194/acp-16-3099-2016

Davidson, E. A., Ishida, F. Y., & Nepstad, D. C. (2004). Effects of an experimental drought on soil emissions of carbon dioxide, methane, nitrous oxide, and nitric oxide in a moist tropical forest. *Global Change Biology*, *10*, 718–730. https://doi.org/10.1111/j.1365-2486.2004.00762.x

Davis, N., & Birner, T. (2017). On the discrepancies in tropical belt expansion between reanalyses and climate models and among tropical belt width metrics. *Journal of Climate*, *30*, 1211–1231. https://doi.org/10.1175/JCLI-D-16-0371.1

Dlugokencky, E. J., Lang, P. M., Crotwell, A. M., & Crotwell, M. J. (2017). Atmospheric methane dry air mole fractions from the NOAA ESRL carbon cycle cooperative global air sampling network, 1983–2016, Version: 2017-07-28. Retrieved from ftp://aftp.cmdl.noaa.gov/data/trace_gases/ch4/flask/surface/

Dlugokencky, E. J., Myers, R. C., Lang, P. M., Masarie, K. A., Crotwell, A. M., Thoning, K. W., et al. (2005). Conversion of NOAA atmospheric dry air CH_4 mole fractions to a gravimetrically prepared standard scale. *Journal of Geophysical Research*, *110*, D18306. https://doi.org/10.1029/2005JD006035

Dlugokencky, E. J., Nisbet, E. G., Fisher, R., & Lowry, D. (2011). Global atmospheric methane in 2010: Budget, changes and dangers. *Philosophical Transactions of the Royal Society*, *369*, 2058–2072. https://doi.org/10.1098/rsta.2010.0341

Dlugokencky, E. J., Steele, L. P., Lang, P. M., & Masarie, K. A. (1994). The growth rate and distribution of atmospheric methane. *Journal of Geophysical Research*, *99*(D8), 17,021–17,043. https://doi.org/10.1029/94JD01245

EDGAR (2017). Janssens-Maenhout, G., et al. EDGAR v4.3.2 Global Atlas of the three major Greenhouse Gas Emissions for the period 1970–2012. *Earth System Science Data Discussions*, 1–55. https://doi.org/10.5194/essd-2017-79, 2017, ESSDD. Retrieved from http://edgar.jrc.ec.europa.eu

Etheridge, D. M., Steele, L., Francey, R. J., & Langenfelds, R. L. (1998). Atmospheric methane between 1000 AD and present: Evidence of anthropogenic emissions and climatic variability. *Journal of Geophysical Research*, *103*, 15,979–15,993. https://doi.org/10.1029/98JD00923

Etminan, M., Myhre, G., Highwood, E. J., & Shine, K. P. (2016). Radiative forcing of carbon dioxide, methane and nitrous oxide: A significant revision of the methane radiative forcing. *Geophysical Research Letters*, *43*, 12,614–12,623. https://doi.org/10.1002/2016GL071930

Feinberg, A. I., Coulon, A., Stenke, A., Schwietzke, S., & Peter, T. (2018). Isotopic source signatures: Impact of regional variability on the $\delta^{13}CH_4$ trend and spatial distribution. *Atmospheric Environment*, *174*, 99–111. https://doi.org/10.1016/j.atmosenv.2017.11.037

Fisher, R., Lowry, D., Wilkin, O., Sriskantharajah, S., & Nisbet, E. G. (2006). High-precision, automated stable isotope analysis of atmospheric methane and carbon dioxide using continuous-flow isotope-ratio mass spectrometry. *Rapid Communications in Mass Spectrometry*, *20*, 200–208. https://doi.org/10.1002/rcm.2300

Fisher, R. E., France, J. L., Lowry, D., Lanoisellé, M., Brownlow, R., Pyle, J. A., et al. (2017). Measurement of the ^{13}C isotopic signature of Northern European wetland methane. *Global Biogeochemical Cycles*, *31*, 605–623. https://doi.org/10.1002/2016GB005504

Fisher, R. E., Sriskantharajah, S., Lowry, D., Lanoisellé, M., Fowler, C. M. R., James, R. H., et al. (2011). Arctic methane sources: Isotopic evidence for atmospheric inputs. *Geophysical Research Letters*, *38*, L21803. https://doi.org/10.1029/2011GL049319

France, J. L., Cain, M., Fisher, R. E., Lowry, D., Allen, G., O'Shea, S. J., et al. (2016). Measurements of $\delta^{13}C$ in CH_4 and using particle dispersion modeling to characterize sources of Arctic methane within an air mass. *Journal of Geophysical Research: Atmospheres.*, *121*, 14,257–14,270. https://doi.org/10.1002/2016JD026006

Francey, R. J., Manning, M. R., Allison, C. E., Coram, S. A., Etheridge, D. M., Langenfelds, R. L., et al. (1999). A history of $\delta^{13}C$ in atmospheric CH_4 from the Cape Grim Air Archive and Antarctic firn air. *Journal of Geophysical Research*, *104*, 23,631–23,643. https://doi.org/10.1029/1999JD900357

Fuglestvedt, J., Rogelj, J., Millar, R. J., Allen, M., Boucher, O., Cain, M., et al. (2018). Implications of possible interpretations of 'greenhouse gas balance' in the Paris Agreement. *Philosophical Transactions of the Royal Society A: Mathematical, Physical and Engineering Sciences*, *376*, 20160445. https://doi.org/10.1098/rsta.2016.0445

Ganesan, A. L., Stell, A. C., Gedney, N., Comyn-Platt, E., Hayman, G., Rigby, M., et al. (2018). Spatially-resolved isotopic source signatures of wetland methane emissions. In *Geophysical Research Letters* (Vol. 45, pp. 3737–3745). https://doi.org/10.1002/2018GL077536

Ganesan, A. L., Rigby, M., Lunt, M., Parker, R. J., Boesch, H., Goulding, N., et al. (2017). Atmospheric observations show accurate reporting and little growth in India's methane emissions. *Nature Communications*, *8*, 836. https://doi.org/10.1038/s41467-017-00994-7

Gedney, N., Cox, P. M., & Huntingford, C. (2004). Climate feedback from wetland methane emissions. *Geophysical Research Letters*, *31*, L20503. https://doi.org/10.1029/2004GL020919

Hausmann, P., Sussmann, R., & Smale, D. (2016). Contribution of oil and natural gas production to renewed increase in atmospheric methane (2007–2014): Top–down estimate from ethane and methane column observations. *Atmospheric Chemistry and Physics*, *16*, 3227–3244. https://doi.org/10.5194/acp-16-3227-2016

Hawkins, E., Ortega, P., Suckling, E., Schurer, A., Hegerl, G., Jones, P., et al. (2017). Estimating changes in global temperatures since the preindustrial period. *Bulletin of the American Meteorological Society*, *98*, 1841–1856. https://doi.org/10.1175/BAMS-D-16-0007.1

Helmig, D., Rossabi, S., Hueber, J., Tans, P., Montzka, S. A., Masarie, K., et al. (2016). Reversal of global atmospheric ethane and propane trends largely due to US oil and natural gas production. *Nature Geoscience*, *9*, 490–495. https://doi.org/10.1038/ngeo2721

Hoesly, R. M., Smith, S. J., Feng, L., Klimont, Z., Janssens-Maenhout, G., Pitkanen, T., et al. (2017). Historical (1750–2014) anthropogenic emissions of reactive gases and aerosols from the Community Emission Data System (CEDS). *Geoscientific Model Development*, *11*, 369–408. https://doi.org/10.5194/gmd-11-369-2018

Holmes, A. J., Roslev, P., McDonald, I. R., Iversen, N., Henriksen, K., & Murrell, J. C. (1999). Characterization of methanotrophic bacterial populations in soils showing atmospheric methane uptake. *Applied and Environmental Microbiology*, *65*, 3312–3398.

Holmes, C. D., Prather, M. J., Søvde, O. A., & Myhre, G. (2013). Future methane, hydroxyl, and their uncertainties: Key climate and emission parameters for future predictions. *Atmospheric Chemistry and Physics*, *13*, 285–302. https://doi.org/10.5194/acp-13-285-2013

Hossaini, R., Chipperfield, M. P., Saiz-Lopez, A., Fernandez, R., Monks, S., Feng, W., et al. (2016). A global model of tropospheric chlorine chemistry: Organic versus inorganic sources and impact on methane oxidation. *Journal of Geophysical Research: Atmospheres*, *121*, 14,271–14,297. https://doi.org/10.1002/2016JD025756

IMBIE (2018). Mass balance of the Antarctic Ice Sheet from 1992 to 2017. *Nature*, *558*, 219–232.

IPCC (2018). Global warming of 1.5°C: A special report on the impacts of global warming of 1.5°C above pre-industrial levels. Summary for policymakers. Draft report, 48th IPCC session, Incheon, Korea, 6 Oct. 2018.

Jiménez-Muñoz, J. C., Mattar, C., Barichivich, J., Santamaría-Artigas, A., Takahashi, K., Malhi, Y., et al. (2016). Record-breaking warming and extreme drought in the Amazon rainforest during the course of El Niño 2015-2016. *Scientific Reports*, *6*, 33130. https://doi.org/10.1038/srep33130

Kirschke, S., Bousquet, P., Ciais, P., Saunois, M., Canadell, J. G., Dlugokencky, E. J., et al. (2013). Three decades of global methane sources and sinks. *Nature Geoscience*, *6*, 813–823. https://doi.org/10.1038/ngeo1955

Lassey, K. R., Etheridge, D. M., Lowe, D. C., Smith, A. M., & Ferretti, D. F. (2007). Centennial evolution of the atmospheric methane budget: What do the carbon isotopes tell us? *Atmospheric Chemistry and Physics*, *7*, 2119–2139. https://doi.org/10.5194/acp-7-2119-2007

Lelieveld, J., Crutzen, P. J., & Dentener, F. J. (1998). Changing concentration, lifetime and climate forcing of atmospheric methane. *Tellus*, *50*, 128–150. https://doi.org/10.1034/j.1600-0889.1998.t01-1-00002.x

Lelieveld, J., Dentener, F. J., Peters, W., & Krol, M. C. (2004). On the role of hydroxyl radicals in the self-cleansing capacity of the troposphere. *Atmospheric Chemistry and Physics*, *4*, 2337–2344. https://doi.org/10.5194/acp-4-2337-2004

Lelieveld, J., Gromov, S., Pozzer, A., & Taraborrelli, D. (2016). Global tropospheric hydroxyl distribution, budget and reactivity. *Atmospheric Chemistry and Physics*, *16*, 12,477–12,493. https://doi.org/10.5194/acp-16-12477-2016

L'Heureux, M. L., Takahashi, K., Watkins, A. B., Barnston, A. G., Becker, E. J., di Liberto, T. E., et al. (2017). Observing and predicting the 2015/6 El Niño. *Bulletin of the American Meteorological Society*, *98*, 1363–1382. https://doi.org/10.1175/BAMS-D-16-0009.1

Lowe, D. C., Brenninkmeijer, C. A. M., Brailsford, G. W., Lassey, K. R., Gomez, A. J., & Nisbet, E. G. (1994). Concentration and ^{13}C records of atmospheric methane in New Zealand and Antarctica: Evidence for changes in methane sources. *Journal of Geophysical Research*, *99*(D8), 16,913–16,925. https://doi.org/10.1029/94JD00908

Mattey, D. P., Fisher, R., Atkinson, T. C., Latin, J. P., Durrell, R., Ainsworth, M., et al. (2013). Methane in underground air in Gibraltar karst. *Earth and Planetary Science Letters*, *374*, 71–80. https://doi.org/10.1016/j.epsl.2013.05.011

Mayfield, E. N., Robinson, A. L., & Cohon, J. L. (2017). System-wide and super-emitter policy options for the abatement of methane emissions from the US natural gas system. *Environmental Science & Technology*, *51*, 4772–4780. https://doi.org/10.1021/acs.est.6b05052

McNorton, J., Chipperfield, M. P., Gloor, M., Wilson, C., Feng, W., Hayman, G. D., et al. (2016). Role of OH variability in the stalling of the global atmospheric CH_4 growth rate from 1999 to 2006. *Atmospheric Chemistry and Physics*, *16*, 7943–7956. https://doi.org/10.5194/acp-16-7943-2016

McNorton, J., Gloor, E., Wilson, C., Hayman, G. D., Gedney, N., Comyn-Platt, E., et al. (2016). Role of regional wetland emissions in atmospheric methane variability. *Geophysical Research Letters*, *43*, 11,433–11,444. https://doi.org/10.1002/2016GL070649

Meinshausen, M., Smith, S. J., Calvin, K., Daniel, J. S., Kainuma, M. L. T., Lamarque, J. F., et al. (2011). The RCP greenhouse gas concentrations and their extensions from 1765 to 2300. *Climate Change*, *109*, 213–241. https://doi.org/10.1007/s10584-011-0156-z

Melton, J. R., Wania, R., Hodson, E. L., Poulter, B., Ringeval, B., Spahni, R., et al. (2013). Present state of global wetland extent and wetland methane modelling: Conclusions from a model intercomparison project (WETCHIMP). *Biogeosciences*, *10*, 753–788. https://doi.org/10.5194/bg-10-753-2013

Millar, R., Fuglestvedt, J. S., Friedlingstein, P., Rogelj, J., Grubb, M. J., Matthews, H. D., et al. (2017). Emission budgets and pathways consistent with limiting warming to 1.5°C. *Nature Geoscience*, *10*, 741–747. https://doi.org/10.1038/ngeo3031

Miller, J. B., Mack, K. A., Dissly, R., White, J. W. C., Dlugokencky, E. J., & Tans, P. P. (2002). Development of analytical methods and measurements of 13C/12C in atmospheric CH_4 from the NOAA climate monitoring and diagnostics laboratory global air sampling network. *Journal of Geophysical Research*, *107*(D13), 4178. https://doi.org/10.1029/2001JD000630

Montzka, S. A., Dutton, G. S., Yu, P., Ray, E., Portmann, R. W., Daniel, J. S., et al. (2018). An unexpected and persistent increase in emissions of ozone-depleting CFC-11. *Nature*, *557*, 413–417. https://doi.org/10.1038/s41586-018-0106-2

Montzka, S. A., Krol, M., Dlugokencky, E., Hall, B., Jockel, P., & Lelieveld, J. (2011). Small interannual variability of global atmospheric hydroxyl. *Science*, *331*, 67–69. https://doi.org/10.1126/science.1197640

Moss, R., Nakicenovic, N., & O'Neill, B. C. (2008). Towards new scenarios for analysis of emissions, climate change, impacts, and response strategies. Intergovernmental panel on climate change (132 pp.). Geneva. Retrieved from http://www.ipcc.ch/pdf/supporting-material/expert-meeting-report-scenarios.pdf

Myhre, C. L., Ferré, B., Platt, S. M., Silyakova, A., Hermansen, O., Allen, G., et al. (2016). Extensive release of methane from Arctic seabed west of Svalbard during summer 2014 does not influence the atmosphere. *Geophysical Research Letters*, *43*, 4624–4631. https://doi.org/10.1002/2016GL068999

Myhre, G., Shindell, D., Bréon, F.-M., Collins, W., Fuglestvedt, J., Huang, J., et al. (2013). Anthropogenic and natural radiative forcing. In T. F. Stocker, et al. (Eds.), *Climate change 2013: The physical science basis. Contribution of working group I to the fifth assessment report of the intergovernmental panel on climate change* (pp. 659–740). Cambridge, UK and New York: Cambridge University Press. https://doi.org/10.1017/CBO9781107415324.018

Naus, S., Montzka, S. A., Pandey, S., Basu, S., Dlugokencky, E. J., & Krol, M. (2019). Constraints and biases in a tropospheric two-box model of OH. *Atmospheric Chemistry and Physics*, *19*, 407–424. https://doi.org/10.5194/acp-19-407-2019

NCDC (2017). *Global climate report – 2017*. US NOAA National centers for environmental information. Retrieved from www.ncdc.noaa.gov/sotc/global/201713

Nicely, J. M., Canty, T. P., Manyin, M., Oman, L. D., Salawitch, R. J., Steenrod, S. D., et al. (2018). Changes in global tropospheric OH expected as a result of climate change over the last several decades. *Journal of Geophysical Research: Atmospheres*, *123*, 10,774–10,795. https://doi.org/10.1029/2018JD028388

Nisbet, E. G., Dlugokencky, E. J., & Bousquet, P. (2014). Methane on the rise—Again. *Science*, *343*, 493–495. https://doi.org/10.1126/science.1247828

Nisbet, E. G., Dlugokencky, E. J., Manning, M. R., Lowry, D., Fisher, R. E., France, J. L., et al. (2016). Rising atmospheric methane: 2007–2014 growth and isotopic shift. *Global Biogeochemical Cycles*, *30*, 1356–1370. https://doi.org/10.1002/2016GB005406

Nisbet, E. G., & Weiss, R. (2010). Top-down vs. bottom-up. *Science*, *328*, 1241–1243. https://doi.org/10.1126/science.1189936

NSIDC (2018). National snow and ice data center. Retrieved from https://nsidc.org/

Obama, B. (2015). A world that is worthy of our children. Remarks at the first session of COP21, Paris, France, 30 Nov. 2015.

Ovando, J., Tomasella, J., Rodriguez, D. A., Martinez, J. M., Siqueira-Junior, J. L., Pinto, G. L. N., et al. (2015). Extreme flood events in the Bolivian Amazon wetlands. *Journal of Hydrology: Regional Studies*, *5*, 293–308.

Parker, R. J., Boesch, H., McNorton, J., Comyn-Platt, E., Gloor, M., Wilson, C., et al. (2018). Evaluating year-to-year anomalies in tropical wetland methane emissions using satellite CH_4 observations. *Remote Sensing of Environment*, *211*, 261–275. https://doi.org/10.1016/j.rse.2018.02.011

Peischl, J., Karion, A., Sweeney, C., Kort, E. A., Smith, M. L., Brandt, A. R., et al. (2016). Quantifying atmospheric methane emissions from oil and natural gas production in the Bakken shale region of North Dakota. *Journal of Geophysical Research: Atmospheres*, *121*, 6101–6111. https://doi.org/10.1002/2015JD024631

Petrenko, V. V., Smith, A. M., Schaefer, H., Riedel, K., Brook, E., Baggenstos, D., et al. (2017). Minimal geological methane emissions during the Younger Dryas–Preboreal abrupt warming event. *Nature*, *548*, 443–446. https://doi.org/10.1038/nature23316

Pitham, F., & Mauritsen, T. (2014). Arctic amplification dominated by temperature feedbacks in contemporary climate models. *Nature Geoscience*, *7*, 181–184. https://doi.org/10.1038/ngeo2071

Poulter, B., Bousquet, P., Canadell, J. G., Ciais, P., Peregon, A., Saunois, M., et al. (2017). Global wetland contribution to 2000–2012 atmospheric methane growth rate dynamics. *Environmental Research Letters*, *12*, 094013. https://doi.org/10.1088/1748-9326/aa8391

Prather, M. J., & Holmes, C. D. (2017). Overexplaining or underexplaining methane's role in climate change. *Proceedings of the National Academy of Sciences*, *114*, 5324–5326. https://doi.org/10.1073/pnas.1704884114

Rahmstorf, S., Foster, G., & Cahill, N. (2017). Global temperature evolution: Recent trends and some pitfalls. *Environmental Research Letters*, *12*, 054001. https://doi.org/10.1088/1748-9326/aa6825

Rhodes, R. H., Brook, E. J., McConnell, J. R., Blunier, T., Sime, L. C., Faïn, X., & Mulvaney, R. (2017). Atmospheric methane variability: Centennial-scale signals in the Last Glacial Period. *Global Biogeochemical Cycles*, *31*, 575–590. https://doi.org/10.1002/2016GB005570

Rice, A. L., Butenhoff, C. L., Teama, D. G., Röger, F. H., Khalil, M. A. K., & Rasmussen, R. A. (2016). Atmospheric methane isotopic record favors fossil sources flat in 1980s and 1990s with recent increase. *Proceedings of the National Academy of Sciences of the United States of America*, *113*, 10,791–10,796. https://doi.org/10.1073/pnas.1522923113

Rigby, M., Montzka, S. A., Prinn, R. G., White, J. W. C., Young, D., O'Doherty, S., et al. (2017). Role of atmospheric oxidation in recent methane growth. *Proceedings of the National Academy of Sciences of the United States of America*, *114*, 5373–5377. https://doi.org/10.1073/pnas.1616426114

Ritchie, H., Reay, D. S., & Higgins, P. (2018). The impact of global dietary guidelines on climate change. *Global Environmental Change*, *49*, 46–55. https://doi.org/10.1016/j.gloenvcha.2018.02.005

Rogelj, J., Meinshausen, M., & Knutti, R. (2012). Global warming under old and new scenarios using IPCC climate sensitivity range estimates. *Nature Climate Change*, *2*, 248–253. https://doi.org/10.1038/nclimate1385

Rogelj, J., Reisinger, A., McCollum, D. L., Knutti, R., Riahi, K., & Meinshausen, M. (2015). Mitigation choices impact carbon budget size compatible with low temperature goals. *Environmental Research Letters*, *10*(7). https://doi.org/10.1088/1748-9326/10/7/075003

Saueressig, G., Crowley, J. N., Bergamaschi, P., Brühl, C., Brenninkmeijer, C. A. M., & Fischer, H. (2001). Carbon 13 and D kinetic isotope effects in the reactions of CH_4 with $O(^1D)$ and OH: New laboratory measurements and their implications for the isotopic composition of stratospheric methane. *Journal of Geophysical Research*, *106*(D19), 23,127–23,138. https://doi.org/10.1029/2000JD000120

Saunois, M., Bousquet, P., Poulter, B., Peregon, A., Ciais, P., Canadell, J. G., et al. (2016). The global methane budget 2000–2012. *Earth System Science Data*, *8*, 697–751. https://doi.org/10.5194/essd-8-697-2016

Saunois, M., Bousquet, P., Poulter, B., Peregon, A., Ciais, P., Canadell, J. G., et al. (2017). Variability and quasi-decadal changes in the methane budget over the period 2000–2012. *Atmospheric Chemistry and Physics*, *17*, 11,135–11,161. https://doi.org/10.5194/acp-17-11135-2017

Saunois, M., Jackson, R. B., Bousquet, P., Poulter, B., & Canadell, J. G. (2016). The growing role of methane in anthropogenic climate change. *Environmental Research Letters*, *11*, 120207. https://doi.org/10.1088/1748-9326/11/12/120207

Schaefer, H., Fletcher, S. E. M., Veidt, C., Lassey, K. R., Brailsford, G. W., Bromley, T. M., et al. (2016). A 21st century shift from fossil-fuel to biogenic methane emissions indicated by $^{13}CH_4$. *Science*, *352*, 80–84. https://doi.org/10.1126/science.aad2705

Schurer, A. P., Cowtan, K., Hawkins, E., Mann, M. E., Scott, V., & Tett, S. F. B. (2018). Interpretations of the Paris climate target. *Nature Geoscience*, *11*, 220–221. https://doi.org/10.1038/s41561-018-0086-8

Schwietzke, S., Pétron, G., Conley, S., Pickering, C., Mielke-Maday, I., Dlugokencky, E. J., et al. (2017). Improved mechanistic understanding of natural gas methane emissions from spatially resolved aircraft measurements. *Environmental Science & Technology*, *51*, 7286–7294. https://doi.org/10.1021/acs.est.7b01810

Schwietzke, S., Sherwood, O. A., Bruhwiler, L. M. P., Miller, J. B., Etiope, G., Dlugokencky, E. J., et al. (2016). Upward revision of global fossil fuel methane emissions based on isotope database. *Nature*, *538*, 88–91. https://doi.org/10.1038/nature19797

Serrano-Silva, N., Sarria-Guzmán, Y., Dendooven, L., & Luna-Guido, M. (2014). Methanogenesis and methanotrophy in soil: A review. *Pedosphere*, *24*, 291–307. https://doi.org/10.1016/S1002-0160(14)60016-3

Sherwood, O., Schwietzke, S., Arling, V. & Etiope, G. Global inventory of fossil and non-fossil methane δ13C source signature measurements for improved atmospheric modeling (2016). http://doi.org/10.15138/G37P4D

Sherwood, O. A., Schwietzke, S., Arling, V. A., & Etiope, G. (2017). Global inventory of gas geochemistry data from fossil fuel, microbial and biomass burning sources, version 2017. *Earth System Science Data Discussions*. https://doi.org/10.5194/essd-2017-20

Shindell, D. T., Fuglestvedt, J. S., & Collins, W. J. (2017). The social cost of methane: Theory and applications. *Faraday Discussions*, *200*, 429–451. https://doi.org/10.1039/C7FD00009J

Spivakovsky, C. M., Logan, J. A., Montzka, S. A., Balkanski, Y. J., Foreman-Fowler, M., Jones, D. B. A., et al. (2000). Three dimensional climatological distribution of tropospheric OH: Update and evaluation. *Journal of Geophysical Research*, *105*(D7), 8931–8980. https://doi.org/10.1029/1999JD901006

Stocker, T. F., Qin, D., Plattner, G.-K., Tignor, M., Allen, S. K., Boschung, J., et al. (2013). *IPCC, 2013: Climate change 2013: The physical science basis*, Contribution of Working Group I to the Fifth Assessment Report of the Intergovernmental Panel on Climate Change (p. 1535). Cambridge, UK and New York: Cambridge University Press.

Stolper, D. A., Martini, A. M., Clog, M., Douglas, P. M., Shusta, S. S., Valentine, D. L., et al. (2015). Distinguishing and understanding thermogenic and biogenic sources of methane using multiply substituted isotopologues. *Geochimica et Cosmochimica Acta*, *161*, 219–247. https://doi.org/10.1016/j.gca.2015.04.015

Sweeney, C., Dlugokencky, E., Miller, C. E., Wofsy, S., Karion, A., Dinardo, S., et al. (2016). No significant increase in long-term CH4 emissions on North Slope of Alaska despite significant increase in air temperature. *Geophysical Research Letters*, *43*, 6604–6611. https://doi.org/10.1002/2016GL069292

Talaiekhozani, A., Bahrami, S., Hashemi, S. M. J., & Jorfi, S. (2016). Evaluation and analysis of gaseous emission in landfill area and estimation of its pollutants dispersion, (case of Rodan in Hormozgan, Iran). *Environmental Health Engineering and Management Journal*, *3*, 143–150. https://doi.org/10.15171/EHEM.2016.13

Tanaka, K., & O'Neill, B. C. (2018). The Paris Agreement zero-emissions goal is not always consistent with the 1.5 °C and 2 °C temperature targets. *Nature Climate Change*, *8*, 319. https://doi.org/10.1038/s41558-018-0097-x–324.

Tans, P. P. (1997). A note on isotopic ratios and the global methane budget. *Global Biogeochemical Cycles*, *11*, 77–81. https://doi.org/10.1029/96GB03940

Thompson, R. L., Nisbet, E. G., Pisso, I., Stohl, A., Blake, D., Dlugokencky, E. J., et al. (2018). Variability in atmospheric methane from fossil fuel and microbial sources over the last three decades. *Geophysical Research Letters*, *45*, 11,499–11,508. https://doi.org/10.1029/2018GL078127

Thompson, R. L., Sasakawa, M., Machida, T., Aalto, T., Worthy, D., Lavric, J. V., et al. (2017). Methane fluxes in the high northern latitudes for 2005-2013 estimated using a Bayesian atmospheric inversion. *Atmospheric Chemistry: Physics*, *17*, 3553–3572. https://doi.org/10.5194/acp-17-3553-2017

Thompson, R. L., Stohl, A., Zhou, L. X., Dlugokencky, E., Fukuyama, Y., Tohjima, Y., et al. (2015). Methane emissions in East Asia for 2000-2011 estimated using an atmospheric Bayesian inversion. *Journal of Geophysical Research: Atmospheres*, *120*, 4352–4369. https://doi.org/10.1002/2014JD022394

Thornton, B. F., Geibel, M. C., Crill, P. M., Humborg, C., & Mörth, C. M. (2016). Methane fluxes from the sea to the atmosphere across the Siberian shelf seas. *Geophysical Research Letters*, *43*, 5869–5877. https://doi.org/10.1002/2016GL068977

Thornton, B. F., Wik, M., & Crill, P. M. (2016). Double-counting challenges the accuracy of high-latitude methane inventories. *Geophysical Research Letters*, *43*, 12,569–12,577. https://doi.org/10.1002/2016GL071772

Trigo, R. M., García-Herrera, R., Díaz, J., Trigo, I. F., & Valente, M. A. (2005). How exceptional was the early August 2003 heatwave in France? *Geophysical Research Letters*, *32*, L10701. https://doi.org/10.1029/2005GL022410

Turner, A. J., Frankenberg, C., Wennberg, P. O., & Jacob, D. J. (2017). Ambiguity in the causes for decadal trends in atmospheric methane and hydroxyl. *Proceedings of the National Academy of Sciences of the United States of America*, *114*(21), 5367–5372. https://doi.org/10.1073/pnas.1616020114

Tyler, S. C., Rice, A. L., & Ajie, H. O. (2007). Stable isotopic ratios in atmospheric CH_4: Implications for seasonal sources and sinks. *Journal of Geophysical Research*, *112*, D03303. https://doi.org/10.1029/2006JD007231

UK Met Office (2018). An overview of global surface temperatures in 2017. Retrieved from https://www.metoffice.gov.uk/research/news/2018/global-surface-temperatures-in-2017

Umezawa, T., Brenninkmeijer, C. A. M., Röckmann, T., van der Veen, C., Tyler, S. C., Fujita, R., et al. (2018). Interlaboratory comparison of δ 13 C and δ D measurements of atmospheric CH 4 for combined use of data sets from different laboratories. *Atmospheric Measurement Techniques*, *11*, 1207–1231. https://doi.org/10.5194/amt-11-1207-2018

UNFCCC (2015). The Paris Agreement. United Nations Framework Convention on Climate Change. Retrieved from http://unfccc.int/paris_agreement/items/9485.php

UNFCCC (2017). Work programme resulting from the relevant requests contained in decision 1/CP.21 (342 kB) (version of 28 November 2016 (rev.)).

USEPA (2012). U.S. Environmental Protection Agency, Global Anthropogenic Non-CO2 Greenhouse Gas Emissions: 1990–2030 (U.S. EPA, 2012).

van der Werf, G. R., Randerson, J. T., Giglio, L., van Leeuwen, T. T., Chen, Y., Rogers, B. M., et al. (2017). Global fire emissions estimates during 1997–2016. *Earth System Science Data*, *9*, 697–720. https://doi.org/10.5194/essd-9-697-2017

van Vuuren, D. P., Edmonds, J., Kainuma, M., Riahi, K., Thomson, A., Hibbard, K., et al. (2011). The representative concentration pathways: An overview. *Climatic Change*, *109*, 5–31. https://doi.org/10.1007/s10584-011-0148-z

Vollmer, M. K., Young, D., Trudinger, C. M., Mühle, J., Henne, S., Rigby, M., et al. (2018). Atmospheric histories and emissions of chlorofluorocarbons CFC-13 (CClF3), ΣCFC-114 ($C_2Cl_2F_4$), and CFC-115 (C_2ClF_5). *Atmospheric Chemistry and Physics*, *18*, 979–1002. https://doi.org/10.5194/acp-18-979-2018

Westerman, P., & Ahring, B. K. (1987). Dynamic of methane production, sulfate reduction and denitrification in a permanently waterlogged alder swamp. *Applied and Environmental Microbiology*, *53*, 2554–2559.

Whitburn, S., van Damme, M., Clarisse, L., Turquety, S., Clerbaux, C., & Coheur, P. F. (2016). Doubling of annual ammonia emissions from the peat fires in Indonesia during the 2015 *El Niño*. *Geophysical Research Letters*, *43*, 11,007–11,014. https://doi.org/10.1002/2016GL070620

White, J., Vaughn, B., & Michel, S. E. (2017). University of Colorado, Institute of Arctic and Alpine Research (INSTAAR), Stable Isotopic Composition of Atmospheric Methane (13C) from the NOAA ESRL Carbon Cycle Cooperative Global Air Sampling Network, 1998–2015, Version: 2017-01-20. Retrieved from ftp://aftp.cmdl.noaa.gov/data/trace_gases/ch4c13/flask/

WMO (2016). The global climate in 2011–2015, World Meteorological Organisation Report WMO-No. 1179 (28 pp.). Geneva.

Wolf, J., Asrar, G. R., & West, T. O. (2017). Revised methane emission factors and spatially distributed annual carbon fluxes for global livestock. *Carbon Balance and Management*, *12*, 16. https://doi.org/10.1186/s13021-017-0084-y

Worden, J. R., Bloom, A. A., Pandey, S., Jiang, Z., Worden, H. M., Walker, T. W., et al. (2017). Reduced biomass burning emissions reconcile conflicting estimates of the post-2006 atmospheric methane budget. *Nature Communications*, *8*, 2227. https://doi.org/10.1038/s41467-017-02246-0

Yin, Y., Chevallier, F., Ciais, P., Broquet, G., Fortems-Cheiney, A., Pison, I., & Saunois, M. (2015). Decadal trends in global CO emissions as seen by MOPITT. *Atmospheric Chemistry and Physics*, *15*, 13,433–13,451. https://doi.org/10.5194/acp-15-13433-2015

Zavala-Araiza, D., Lyon, D. R., Alvarez, R. A., Davis, K. J., Harriss, R., Herndon, S. C., et al. (2015). Reconciling divergent estimates of oil and gas methane emissions. *Proceedings of the National Academy of Sciences of the United States of America*, *112*, 15,597–15,602. https://doi.org/10.1073/pnas.1522126112

Zazzeri, G., Lowry, D., Fisher, R. E., France, J. L., Lanoisellé, M., Kelly, B. F. J., et al. (2016). Carbon isotopic signature of coal-derived methane emissions to atmosphere: From coalification to alteration. *Atmospheric Chemistry and Physics*, *16*, 13,669–13,680. https://doi.org/10.5194/acp-16-13669-2016

Zazzeri, G., Lowry, D., Fisher, R. E., France, J. L., Lanoisellé, M., & Nisbet, E. G. (2015). Plume mapping and isotopic characterisation of anthropogenic methane sources. *Atmospheric Environment*, *110*, 151–162. https://doi.org/10.1016/j.atmosenv.2015.03.029

Zhang, Z., Zimmermann, N. E., Stenke, A., Li, X., Hodson, E. L., Zhu, G., et al. (2017). Emerging role of wetland methane emissions in driving 21st century climate change. *Proceedings of the National Academy of Sciences of the United States of America*, *114*(36), 9647–9652. https://doi.org/10.1073/pnas.1618765114

Zimmermann, P. H., Brenninkmeijer, C. A. M., Pozzer, A., Jöckel, P., Zahn, A., Houweling, S., & Lelieveld, J. (2018). Model simulations of atmospheric methane and their evaluation using AGAGE/NOAA surface- and IAGOS-CARIBIC aircraft observations, 1997-2014. *Atmospheric Chemistry and Physics Discussions*, 1–45. https://doi.org/10.5194/acp-2017-1212

Zona, D., Gioli, B., Commane, R., Lindaas, J., Wofsy, S. C., Miller, C. E., et al. (2016). Cold season emissions dominate the Arctic tundra methane budget. *Proceedings of the National Academy of Sciences of the United States of America*, *113*, 40–45. https://doi.org/10.1073/pnas.1516017113

References From the Supporting Information

Burkholder, J. B., Sander, S. P., Abbatt, J. P. D., Barker, J. R., Huie, R. E., Kolb, C. E., et al. (2011). Chemical kinetics and photochemical data for use in atmospheric studies, Evaluation 17, Jet Propulsion Laboratory, Publication 10–16 Pasadena, CA. Retrieved from http://jpldataeval.jpl.nasa.gov/pdf/JPL%2010-6%20Final%2015June2011.pdf

Ferretti, D. F., Miller, J. B., White, J. W., Etheridge, D. M., Lassey, K. R., Lowe, D. C., et al. (2005). Unexpected changes to the global methane budget over the past 2000 years. *Science*, *309*, 1714–1717. https://doi.org/10.1126/science.1115193

Markwardt, C. B. (2009). Non-linear least squares fitting in IDL with MPFIT. In D. Bohlender, P. Dowler, & D. Durand (Eds.), *Astronomical data analysis software and systems XVIII*, *ASP Conference Series* (Vol. 411, pp. 251–254). San Francisco: Astronomical Society of the Pacific.

Masarie, K. A., & Tans, P. P. (1995). Extension and integration of atmospheric carbon dioxide data in a globally consistent measurement record. *Journal of Geophysical Research*, *100*, 11,593–11,610. https://doi.org/10.1029/95JD00859

Miller, S. M., Michalak, A. M., & Levi, P. J. (2014). Atmospheric inverse modeling with known physical bounds: An example from trace gas emissions. *Geoscientific Model Development*, *7*, 303–315. https://doi.org/10.5194/gmd-7-303-2014

NOAA (2018). Global greenhouse gas reference network: Data archive, greenhouse gases. Retrieved from ftp://aftp.cmdl.noaa.gov/data/greenhouse_gases/

Sander, S. P., Abbatt, J., Barker, J. R., Burkholder, J. B., Friedl, R. R., Golden, D. M., et al. (2011). Chemical kinetics and photochemical data for use in atmospheric studies: Evaluation number 17, JPL Publication 10-6, Jet Propulsion Laboratory, Pasadena, CA. Retrieved from http://jpldataeval.jpl.nasa.gov